# A problem-independent limiter for high-order

# Runge-Kutta Discontinuous Galerkin Methods

A. Burbeau[†,1], P. Sagaut[†,2] and Ch.-H. Bruneau[⋆,3]

[†] *ONERA, BP 72 - 29, av. de la Division Leclerc,92322 Châtillon Cedex, FRANCE*
[⋆] *Université Bordeaux I, 351, Cours de la Libération, 33405 Talence Cedex, FRANCE*

E-mail: [1] burbeau@onera.fr; [2] sagaut@onera.fr; [3] bruneau@math.u-bordeaux.fr

*Proposed running head* : SHOCK CAPTURING WITH RKDG METHODS

*Person to whom correspondence should be addressed* :

Pierre Sagaut

ONERA

BP 72 - 29 av. de la Division Leclerc

92322 Châtillon Cedex, FRANCE

sagaut@onera.fr

Tel : (33)-01-46-73-42-71

Fax : (33)-01-46-73-41-66

## 1. INTRODUCTION

A wide range of numerical methods has been developed for the resolution of nonlinear conservation laws. In particular, Direct Numerical Simulation of compressible flows is a real stake. It is then crucial to derive effective methods, able to capture accurately real flows including strong shocks.

This paper deals with high-order discretization methods for convection-dominated problems on unstructured meshes. In this field, Runge-Kutta Discontinuous Galerkin methods (RKDG) have raised up a great interest during the last twenty years. They combine the basis of the Finite Volume and the Finite Element methods, and Riemann problems taking into account the physics of wave propagation. The accuracy is then obtained by means of high-order polynomial within elements. These methods are famous for their formal high-order space and time accuracy, their capacity to handle complicated geometries, their high parallelizability and their nice stability properties.

The first analysis of the method, elaborated by Reed and Hill [30], has been performed by Lesaint and Raviart [26], for a linear transport equation. The adaptation of the scheme to the nonlinear case, which gives rise to the problem of stability, has been first carried out by Chavent and Salzano [10]. They proposed an explicit version of Discontinuous Galerkin method. It deals with a linear spatial discretization and an Euler Forward time discretization method. The main drawback of the method was its bad stability properties (it was stable under a very restrictive CFL condition). Then, the method has been modified by Chavent and Cockburn [9], by the introduction of a local projection operator (a slope limiter), designed

to improve its stability properties. The resulting scheme was proven to be Total Variation Diminishing in the Means (TVDM) and Total Variation Bounded (TVB) under a fixed CFL (less than or equal to 1/2). Unfortunately, the scheme is only first-order accurate in time and the solution is affected in smooth regions.

This history is recalled to introduce the RKDG scheme, developed by Cockburn and Shu in a serie of papers [12, 13, 15]. Their investigations into Runge-Kutta type discretization in time for Discontinuous Galerkin methods, and slope limiters that maintain the formal accuracy of the scheme extrema have helped to improve the efficiency of these methods. It gave rise to RKDG method of arbitrary order of accuracy both in space and time. For the one dimensional case, the scheme was proven to be TVB. Jiang and Shu [25] proved a cell entropy inequality for arbitrary order of accuracy and arbitrary triangulations. The RKDG method has been extended by Cockburn *et al.* [14, 17] to multidimensional systems, for rectangular and triangular elements. They proved a maximum principle for general non linearities and arbitrary triangulations.

The efficiency of the RKDG method has been widely illustrated by many authors. Indeed, it has been tested successfully by Lomtev, Quillen and Karniadakis [28] and Sherwin and Karniadakis [32, 33, 34], for the compressible Euler and Navier-Stokes equations. They coupled the method with a spectral orthogonal and hierarchical set of basis functions due to Dubiner [21]. Numerical simulations with RKDG methods have been also done by Bassi and Rebay [3] who proposed a mixed formulation to discretize the viscous terms. Biswas, Devine and Flaherty [6] used the present method to achieve parallel adaptive refinement for conservation laws. For more details on the use of RKDG methods, see for example the introduction of [11] and

[19, 20, 24, 7].

Besides being of arbitrary order of accuracy, RKDG methods are very attractive for shock-capturing. Indeed, the discontinuous representation of the solution and the upwind flux processing make the scheme well adapted to solutions with discontinuities. When combined with a stabilization technique that prevents spurious oscillations near solution discontinuities, the resulting scheme well captures strong gradients. Several forms of nonlinear limiting have been carried out so as to ensure solution boundedness when discontinuities are present in the flow field. These techniques can be splitted into two classes : one way consists in supplementing the numerical scheme with a viscosity term (see [4]), another one is concerned with the elaboration of a projection procedure to enforce the nonlinear stability. Cockburn and Shu have precisely contributed a lot in the construction of a slope limiter which is applied to the numerical solution given by RKDG method at each time iteration [12, 13, 14, 15, 17]. Let us briefly describe the core of their work. The slope limiting is based on piecewise linear approximations. They assume that spurious oscillations are present in the approximate solution only if they are present in its $P^1$ part. In regions where limiting is necessary, the expansion is then truncated to second order. This technique performs very well in practice (see for example [13]). The high-order accuracy is preserved at local extrema by using a modified minmod function, instead of the classical one, as in the initial version of the slope limiting -It comes to replace TVDM by TVBM property-. However, the projection is problem-dependent due to the presence of a constant, whose aim is to enforce the TVBM property. In addition, as the method is based on second-order approximations, we

can suppose that it gives rise to a lack of information for high-order Discontinuous

Galerkin methods, once the development is locally reduced to a linear term.

Biswas *et al.* [6] proposed an extension of the method of Cockburn and Shu to higher

orders of accuracy, for one-dimensional and two-dimensional rectangular meshes.

The method is based on the $P^1$ TVDM version of Cockburn's slope limiting (which

is a very diffusive procedure), and on a Legendre polynomials basis.

The discontinuous Galerkin approach is not the only existing method which can

be high-order accurate in smooth regions and nonoscillatory near solution disconti-

nuities. For example, the ENO and WENO schemes (see for example [22][1][23]) are

based on high-order polynomial reconstructions and use an adaptive stencil which

permits to avoid interpolation accross discontinuities. In [38], Suresh and Huynh

construct a new class of scheme : a high-order interface polynomial value is first

reconstructed by using a centered stencil. Next, the interface value is limited in or-

der the scheme to satisfy the monotonicity preserving property. A test determines

whether the limiting procedure is needed or not, and then accuracy near extrema

is preserved in all norms. The limiter is problem-independent. However, only one-

dimensional or two-dimensional cartesian meshes are considered, and the stencil is

all the wider as the polynomial degree is high. It can give rise to difficulties in the

boundary conditions treatment.

The case of unstructured grid of triangles is treated in [40]. Wierse proposes a new

limiter function for second-order finite volume schemes. A proof of a maximum

principle is given, for which no requirements on the domain discretization are nec-

essary. It is shown how to adapt this proof to the case of $P^1$ discontinuous Galerkin

approximations.

The aim of the present work is to propose a new slope limiter for discontinuous Galerkin methods of any order of accuracy, which satisfies the following properties :

1. it is totally free of problem-dependence,

2. unstructured triangular meshes can be treated,

3. it suppresses spurious oscillations near solution discontinuities,

4. no loss of accuracy takes place at extrema in the $L^1$-norm,

5. the stencil is restricted to one triangle and its neighboors whatever the order of accuracy is.

The guiding principles in those investigations are based on the papers by Cockburn and Shu [12, 13, 14, 15, 17], and by Biswas *et al.* [6] which provide a frame of reference for the present work.

The paper is organized as follows. Section 2 deals with one-dimensional problems. The necessary background is reviewed, namely : the description of Cockburn's limiting procedure for linear approximations, its extension by Biswas *et al.* to the case of any-order of accuracy. In part two of this section, the proposed limiter is detailled. Numerical results illustrate its good behaviour, for any kind of solutions (regular or with discontinuities).

Section 3 presents the extension of the new limiting procedure to triangular meshes, for the set of basis functions of Dubiner and in the case of $P^1$ and $P^2$ approximations.

## 2. THE DISCONTINUOUS GALERKIN METHOD WITH SLOPE

## LIMITER IN ONE DIMENSION

### 2.1. Outline of the Discontinuous Galerkin Method

In this section, the RKDG method is briefly introduced for the following one-dimensional scalar conservation law :

$$\frac{\partial u}{\partial t} + \frac{\partial f(u)}{\partial x} = 0 \text{ in } \Omega \times (0, T), \ \Omega \subset \mathcal{R} \tag{1}$$

subject to the initial condition

$$u(x, t = 0) = u_0 \ , \ \forall x \in \Omega \tag{2}$$

and periodic boundary conditions.

Let $\{I_j\}_{j=1 \cdots J}$ with $I_j = \left(x_{j-1/2}, x_{j+1/2}\right)$ be a partition of the interval $\Omega$ into subintervals. Let us define

$$V_h = \{p \in BV(\Omega) \cap L^1(\Omega) \ : \ p_{|I_j} \in P^k(I_j)\} \tag{3}$$

where $P^k(I)$ denotes the space of polynomials in $I$ of degree at most $k$ and $BV$ the space of functions with bounded variation. Let

$$\mathcal{B}_j = \{v_{l,j}(x); l = 1, \cdots, k+1\}$$

be the basis of Legendre polynomials on $I_j$.

For each time $t \in [0, T]$, an approximate solution $u_h(t)$ that belongs to $V_h$ is computed. A weak formulation of the problem is obtained by multiplying (1) by a test function $\varphi$. The result is integrated on $I_j$, and the flux term is integrated by part to yield :

$$
\begin{aligned}
&\int_{I_j} \partial_t u(x,t) \varphi(x) dx - \int_{I_j} f(u(x,t)) \partial_x \varphi(x) dx \\
&+ f(u(x_{j+1/2},t)) \varphi(x_{j+1/2}^-) - f(u(x_{j-1/2},t)) \varphi(x_{j-1/2}^+) = 0
\end{aligned}
\tag{4}
$$

where $\varphi(x_{j+1/2}^-)$ and $\varphi(x_{j-1/2}^+, t)$ are the values of function $\varphi$, at interfaces $x_{j\pm 1/2}$ of interval $I_j$.

A discrete analogous of (4) is obtained by replacing the exact solution $u(x,t)$ by the approximation $u_h(x,t)$ and the test function $\varphi$ by each element of the basis set $\mathcal{B}_j$ successively.

The approximate solution can be written as :

$$
u_h(x,t)_{|I_j} = \sum_{l=1}^{k+1} u_{l,j}(t) v_{l,j}(x) \quad \forall \ x \in I_j
\tag{5}
$$

where $\{u_{l,j}\}_{l=1}^{k+1}$ are the degrees of freedom of $u_h$ in the interval $I_j$.

Taking $\varphi = v_{m,j}$ leads to :

$$
\begin{aligned}
&\int_{I_j} \left( \sum_{l=1}^{k+1} \frac{d}{dt} u_{l,j}(t) v_{l,j}(x) \right) v_{m,j}(x) dx - \int_{I_j} f(u_h(x,t)) \frac{d}{dx} v_{m,j}(x) dx \\
&+ h(u_h)_{j+1/2} v_{m,j}(x_{j+1/2}^-) - h(u_h)_{j-1/2} v_{m,j}(x_{j-1/2}^+) = 0
\end{aligned}
\tag{6}
$$

Since solution discontinuities are permitted at element interfaces, the boundary

flux $f(u_h(x_{j+1/2}, t))$ is not uniquely defined. It is then approximated by a numerical

flux function $h$ that depends on the two values of $u_h$ at the point $(x_{j+1/2}, t)$ :

$$h_{j+1/2} = h(u_h)_{j+1/2} = h(u_{j-1/2}^+, u_{j+1/2}^-) \qquad (7)$$

with $u_{j\pm 1/2}^\pm = u_h\left(x_{j\pm 1/2}^\pm\right)$.

The discrete weak formulation yields, by using orthogonality property of $\mathcal{B}_j$ :

$$\frac{d}{dt} u_{m,j}(t)\left(\int_{I_j} v_{m,j}(x)^2 dx\right) = \int_{I_j} f\left(\sum_{l=1}^{k+1} u_{l,j}(t)v_{l,j}(x)\right)\frac{d}{dx}v_{m,j}(x)dx$$
$$-h_{j+\frac{1}{2}}v_{m,j}(x_{j+\frac{1}{2}}^-) + h_{j-\frac{1}{2}}v_{m,j}(x_{j-\frac{1}{2}}^+) \qquad (8)$$

where the integral term on the right-hand side is evaluated using Gauss quadra-

ture.

At last, the following ODE is obtained :

$$\frac{d}{dt}(u_h) = L_h(u_h) \qquad (9)$$

For a complete discussion of the method, the reader is refered to [11].

## 2.2.    Existing stabilization techniques

The approach in this section is to describe firstly the limiting procedure by Cock-

burn and Shu, and secondly the generalization of the method to $P^k$ approximations.

It relies on the construction of a slope limiter $\Lambda\Pi_h$ whose aim is to enforce nonlinear

stability properties.

The TVD Runge-Kutta time discretization introduced in [36] is used to integrate the ODE system (9) in time. It is of great importance for the method to be correctly stabilized.

Let $\{t^n\}_{n=0}^N$ be a partition of $[0, T]$. The Runge-Kutta algorithm reads as follows :

1. Set $u_h^0 = \Lambda \Pi_h (u_{0h})$;

2. For $n = 0, \cdots, N - 1$ compute $u_h^{n+1}$ from $u_h^n$ as follows :

    (i) Set $u_h^{(0)} = u_h^n$;

    (ii) For $i = 1, \ldots, I + 1$ compute the intermediate functions :

$$u_h^{(i)} = \sum_{l=0}^{i-1} \Lambda \Pi_h \left( \alpha_{il} u_h^{(l)} + \beta_{il} \Delta t L_h (u_h^{(l)}) \right)$$

    (iii) Set $u_h^{n+1} = u_h^{(I+1)}$

When the projection $\Lambda \Pi_h$ is set equal to the identity operator, the RKDG scheme without slope limiter is recovered. Thanks to this kind of time discretization, good nonlinear stability properties can be obtained [11].

The mesh size $\Delta x$ is assumed to be constant for sake of clarity. For the one-dimensional case, the solution is approximated by :

$$u_{h_{|I_j}} = u_{1,j} + \frac{2}{\Delta x} (x - x_j) u_{2,j} = \overline{u}_j + \frac{2}{\Delta x} (x - x_j) u_{2,j} \qquad (10)$$

where the degrees of freedom of $u_h$ are $u_{1,j}$ and $u_{2,j}$, which are respectively designed for the approximation of the mean value of the solution (denoted by $\overline{u}_j$) and of the solution gradient on the interval $I_j$.

The slope limiter $\Lambda\Pi_h$ must :

(i) maintain the conservation of mass element by element,

(ii) not degrade the accuracy of the method,

(iii) decrease the gradient of the resulting approximate solution that must be less or equal to those issued from discontinuous Galerkin space discretization.

The following generalized slope limiter, proposed by Cockburn and Shu, does satisfy such conditions :

$$\Lambda\Pi_h\, u_h \;=\; \widetilde{u}_h \;=\; \overline{u}_j + \frac{2}{\Delta x}\left(x - x_j\right)\tilde{u}_{2,j}$$

$$=\; \overline{u}_j + \frac{2}{\Delta x}(x - x_j)\ \mathrm{minmod}\left(u_{2,j}, \overline{u}_{j+1} - \overline{u}_j, \overline{u}_j - \overline{u}_{j-1}\right)\ \forall x \in I_j \tag{11}$$

where the minmod function is defined as follows :

$$\mathrm{minmod}(a_1, \ldots, a_m) = \begin{cases} s\ \min_{1 \le n \le m}|a_n|, \ \text{if}\ s = sign(a_1) = \ldots = sign(a_m), \\[2ex] 0,\ \text{otherwise} \end{cases} \tag{12}$$

Equation (11) can be rewritten as :

$$
\begin{cases}
\tilde{u}_{j+1/2}^{-} = \overline{u}_j + \text{minmod}\left(u_{j+1/2} - \overline{u}_j, \overline{u}_{j+1} - \overline{u}_j, \overline{u}_j - \overline{u}_{j-1}\right) \\
\\
\tilde{u}_{j-1/2}^{+} = \overline{u}_j - \text{minmod}\left(\overline{u}_j - u_{j-1/2}, \overline{u}_{j+1} - \overline{u}_j, \overline{u}_j - \overline{u}_{j-1}\right)
\end{cases}
\tag{13}
$$

The resulting RKDG scheme with the slope limiter previously described is proven to be TVDM. It can be rendered TVBM by modifying the minmod function (see [12]) so as not to degrade accuracy at local extrema. Then, it relies on the introduction of a constant $M$, which is an upper bound of the absolute value of the solution second order derivative at local extrema. The TVB corrected minmod function $\overline{m}$ is defined as follows :

$$
\overline{m}(a_1, \ldots, a_m) = \begin{cases}
a_1 & \text{, if } |a_1| \leq M\left(\Delta x\right)^2 \\
\\
\text{minmod}(a_1, \ldots, a_m) & \text{, otherwise}
\end{cases}
\tag{14}
$$

This way, $\tilde{u}_h$ is defined in a unique manner for $P^k$ approximations with $k \leq 2$. For greater values of $k$, Cockburn and Shu suggest to set $\tilde{u}_{l,j} = 0 \ \forall l > 3$. In other words, in regions where limiting is necessary, the development of the numerical solution is locally truncated. The very interesting property of such a method is that no loss of accuracy takes place at extrema, even in the uniform norm. However, the difficulty lies in the evaluation of the constant. Indeed, it can be trivially evaluated in some cases (for example for a piecewise $C^2$ initial data), but there are some problems for which it is not easy to determine.

The extension by Biswas, Devine and Flaherty of this method to the case of higher-order slope limiting is of great interest. The paper [6] contains numerical

results which point out that their proposed limiting projection doesn't destroy high-order accuracy where the solution is very smooth. Furthermore, in practice, solution boundedness is ensured near solution discontinuities. It relies on the TVDM version of the Cockburn and Shu method, and consists in successively differentiating the numerical solution. The result of this derivation procedure gives a linear term which can be treated like in the case of a linear approximation.

Let $\xi \in [-1, +1]$ be the reference element. Noting that for Legendre polynomials :

$$\frac{\partial^l}{\partial \xi^l} u_{h_{|I_j}} = \prod_{m=1}^{l} (2m-1) u_{l,j} + \prod_{m=1}^{l+1} (2m-1) u_{l+1,j} \xi$$
$$+ \sum_{m=l+2}^{k+1} u_{m,j}(t) \frac{d^l}{d\xi^l} v_{m,j}(\xi) \tag{15}$$

The limited approximation is written :

$$\Lambda \Pi_h u_h(x,t)_{|I_j} = \sum_{l=1}^{k+1} \tilde{u}_{l,j}(t) v_{l,j}(x) \quad \forall \, x \in I_j \tag{16}$$

whose degrees of freedom are defined by :

$$\tilde{u}_{l+1,j} = \frac{1}{2l+1} \text{minmod}((2l+1) u_{l+1,j}, u_{l,j+1} - u_{l,j}, u_{l,j} - u_{l,j-1}), \text{ for } l = 1, \cdots, k$$
$$\tag{17}$$

In practice, following Biswas, the limiter is applied adaptively. The highest-order coefficient is first limited. The limiter is then applied to successively lower-order coefficients when the next higher-coefficient on the interval is changed by the lim-

iting. This is a way to maintain accuracy in smooth regions, and to apply limiting procedure only where it is needed. A comprehensive treatment of the method can be found in [6]. For vector systems, the limiter is applied to the characteristic fields of the system.

An improved limiter is proposed in the next section. The resulting method is less diffusive near solution discontinuities and still keeps a good level of accuracy in regions where the solution is smooth.

### 2.3. A new slope limiter for one-dimensional problems

There are two key points to ensure the success of a limiting procedure. Firstly, as it is crucial to preserve the accuracy of RKDG method in smooth regions, a criterion is necessary to determine regions where the approximate solution must be limited. This is exactly the aim of the constant $M$ introduced by Cockburn and Shu in the modified minmod function. Another criterion is proposed in what follows. It is free of problem-dependence. Secondly, when limiting, it is necessary to introduce enough numerical diffusion to stabilize the method. However, a too large amount of viscosity can flatten extrema. Then, a way to balance these two points must be found out.

Due to the differentiation procedure, the method is suited for any order of accuracy once the projection is defined for a linear approximation. In the present section, a new method is proposed, which combines a basic idea due to Van Leer

[39] and the method previously described.

We first address the problem of the definition of a regularity criterion. One interesting idea concerning the slope limiter previously described relies on the fact that in regions where the solution is smooth, we have $\tilde{u}_{2,j} = u_{2,j}$, which means that the projection $\Lambda\Pi_h$ has no effect on $u_h$ (it is locally reduced to Identity operator). Consequently,

$$\tilde{u}_{2,j} = \text{minmod}\left(u_{2,j}, \overline{u}_{j+1} - \overline{u}_j, \overline{u}_j - \overline{u}_{j-1}\right) \tag{18}$$

will be used as a regularity criterion. In other words, "large" gradients are those for which $\tilde{u}_{2,j} \neq u_{2,j}$.

It remains to define the limiting procedure. The main drawback of (18) appears on regular extrema which are flattened. This problem is resolved by relaxing the limitation procedure as follows :

$$
\begin{cases}
u_{2,j}^m & = \ \text{minmod}\left(u_{j+1/2}^- - \overline{u}_j, \ \overline{u}_{j+1} - \overline{u}_j, \ \overline{u}_j - \overline{u}_{j-1}\right) \\[2em]
u_{2,j}^{max} & = \ \text{minmod}\left(u_{j+1/2}^+ - \overline{u}_j, \ u_{j+1/2}^- - \overline{u}_j, \ \overline{u}_j - u_{j-1/2}^-\right) \\[2em]
\tilde{u}_{2,j} & = \ \text{maxmod}\left(u_{2,j}^m, \ u_{2,j}^{max}\right)
\end{cases}
\tag{19}
$$

with the definition of maxmod function :

$$\text{maxmod}(a_1, \ldots, a_m) = \begin{cases} s \ \max_{1 \le n \le m}|a_n|, \text{ if } s = sign(a_1) = \ldots = sign(a_m), \\ \\ 0, \text{ otherwise} \end{cases}$$

$$(20)$$

Solution gradients at interfaces of each cell are then evaluated by two different ways, and the gradient which less restricts the approximate gradients coming from the discontinuous Galerkin method is retained.

A very simple example of the projection effects on two configurations is proposed, in order to understand the action of (19) . The projection's results for an extremum are explained by referring to Figure 1. While the minmod function is inclined to flatten the smooth extremum, the maxmod function (19) doesn't. Besides, the proposed limiter correctly suppresses spurious oscillations (as illustrated by the example of non-smooth extremum).

The previous method is generalizable to $P^k$ approximations. A regularity criterion is associated to each degree of freedom to determine whether it should be limited or not.

For $j = 1, \cdots, N$ and $l = k, \cdots, 1$, we define

$$u_{l+1,j}^m = \frac{1}{2m+1}\text{minmod}((2l + 1)u_{l+1,j}, u_{l,j+1} - u_{l,j}, u_{l,j} - u_{l,j-1}) \qquad (21)$$

If $u_{l+1,j}^m = u_{l+1,j}$ then

$$\Lambda \Pi_h u_{h_{|_{I_j}}} = \sum_{s=1}^{l+1} u_{s,j} v_{s,j} + \sum_{s=l+2}^{k+1} \tilde{u}_{s,j} v_{s,j} \tag{22}$$

else

$$\tilde{u}_{l+1,j} = \mathrm{maxmod}\left(u_{l+1,j}^m, u_{l+1,j}^{max}\right) \tag{23}$$

where

$$u_{l+1,j}^{max} \quad = \quad \frac{1}{2m+1} \mathrm{minmod}((2l+1)u_{l+1,j}, w_{l,j+1/2}^+ - u_{l,j}, u_{l,j} - w_{l,j-1/2}^-)$$

$$w_{l,j+1/2}^+ \quad = \quad u_{l,j+1} - (2l+1)u_{l+1,j+1}$$

$$w_{l,j-1/2}^- \quad = \quad u_{l,j-1} + (2l+1)u_{l+1,j-1}$$

and the limiting procedure goes on.

### 2.4.    Numerical results

*2.4.1.   Accuracy test for RKDG method with slope limiter*

Two test problems are proposed to illustrate the effective order of convergence of the method (a $k+1$ rate of convergence is expected for a $P^k$ approximation). Both are related to the linear scalar transport equation :

$$\begin{cases} u_t + u_x & = \ 0 \ \ , \ -1 \le x \le 1 \\ u(x,0) & = \ u_0(x) \end{cases} \tag{24}$$

with periodic boundary conditions.

Tables I and II show the errors for the initial condition $u_0(x) = \sin(\pi x)$ at time t=1. The results obtained with the unlimited DG method are compared with the errors of the limited scheme with the Biswas *et al.* limiter (denoted by DG$^{\min}$ where min stands for minmod) and the new one (denoted by DG$^{\max}$ for maxmod). Both of the DG$^{\min}$ and the DG$^{\max}$ methods do not affect the rate of convergence of the scheme in the $L^1$-norm, but a loss of accuracy shows up in the $L^\infty$-norm (around half a power of the rate of convergence is lost).

A much tougher case is now considered with the initial condition $u_0(x) = \sin^4(\pi x)$. Results at time t=1 are summarized in Tables III and IV. The limiters still keep the high order of accuracy.

### 2.4.2. Riemann problems of nonlinear conservation law system

The system of Euler equations is now considered. The first selected test case is Sod's problem with initial conditions

$$
\begin{aligned}
\mathbf{U} &= [\rho_L, u_L, p_L]^T &= [1, 0, 1], && \text{if } 0 \le x \le 0.5 \\
&= [\rho_R, u_R, p_R]^T &= [0.125, 0, 0.1], && \text{if } 0.5 \le x < 1
\end{aligned}
\tag{25}
$$

The results can be compared for example with those of Ref. [13].

As illustrated by Figures 2 and 3, the proposed limiter is suitable for scalar one-dimensional hyperbolic conservation laws with discontinuities. For linear approximations, it performs very well, despite the fact that the maxmod function authorizes greater gradients than the initial minmod function. The $P^2$ version of the

limiter is also well adapted for shock-capturing, since oscillations are not developed.

The next test case concerns initial conditions

$$
\begin{aligned}
\mathbf{U} &= [\rho_L, u_L, p_L]^T &&= [3.857143, 2.629369, 10.333333], && \text{when } x < -4 \\
&= [\rho_R, u_R, p_R]^T &&= [1 + 0.2 sin(5x), 0, 1], && \text{when } x \geq -4
\end{aligned}
\tag{26}
$$

This test problem, elaborated by Shu and Osher [37], is well adapted to demonstrate the advantage of higher-order methods since the solution has smooth structures interspersed with discontinuities. The results obtained with the proposed method are shown in Figures 4 and 5. It is clear that the $P^2$ version of slope limiter performs much better than the linear one. The improvement due to the fourth-order accuracy is also seen. Furthermore, the proposed limiter is seen to improve significantly the results obtained using the Biswas *et al.* limiter -see Figure 5 for fourth-order of accuracy-. A similar behavior is observed for any order of approximation. The introduction of the maxmod function leads to much less diffusive results whatever the order of accuracy is.

In summary, the accuracy is maintained in regions where the solution is smooth. The projection $\Lambda\Pi_h$ of course leads to additional error but does not reduce the order of convergence of RKDG scheme. This is accomplished in a fully problem-independent way.

On the other hand, the numerical solution is getting better and better in the neighbourhood of the solution's discontinuity, when the degree of the polynomial $k$ is

increased.

## 3.   EXTENSION TO MULTIDIMENSIONAL SYSTEMS

The adaptation of the method to multidimensional unstructured meshes raises numerous problems, among them the problem of stability. This section presents the extension to triangular meshes of the new stabilization method described for one-dimensional problems. To achieve that, we take advantage of the paper by Cockburn and Shu [17] which contains an adaptation of their slope limiter to the case of unstructured grids for linear approximations. After the description of the process for $P^1$ approximations, the $P^2$ case is considered.

### 3.1.   The Dubiner set of basis functions

We start by introducing useful notations.

Let $\mathcal{T}_h$ be a triangulation of $\Omega$. The approximate solution $\mathbf{U}_h(\mathbf{x}, t)$, for fixed $t \in [0, T]$, belongs to the finite dimensional space :

$$V_h = \{v_h \in L^\infty(\Omega) : \ v_{h|_T} \in V(T), \forall T \in \mathcal{T}_h\} \tag{27}$$

where $V(T)$ is a space locally defined. We take $V(T) = P^k(T)$.

The approximate vector solution $\mathbf{U}_h$ is expressed as follows :

$$\mathbf{U}_h(\mathbf{x}, t) = \sum_{i=1}^{n} \mathbf{U}_i(t)\Phi_i(\mathbf{x}) \quad \forall \mathbf{x} \in T \tag{28}$$

where $\mathbf{U}_i(t)$ are the degrees of freedom and $\{\Phi_i\}_{i=1}^n$ a basis for $V(T)$.

The scheme implementation can be made more effective thanks to the choice of the polynomial basis. In accordance with the papers by Sherwin and Karniadakis [32, 33, 34], a spectral basis developed by Dubiner [21] is used. It is recalled in what follows.

The following standard triangle and quadrilateral are considered

$$\hat{T} = \{\ (r,s),\ -1 \le r,s\ ;\ r+s \le 0\} \tag{29}$$

and

$$\hat{R} = \{\ (a,b),\ -1 \le a,b \le +1\} \tag{30}$$

The basis functions can equivalently be written in $\hat{T}$ or $\hat{R}$ thanks to the transforms (see Figure 6) :

$$\hat{T} \quad \longrightarrow \quad \hat{R}$$

$$\mathcal{F}_{\hat{T}/\hat{R}}\ :$$

$$(r,s) \quad \longrightarrow \quad \begin{cases} a & = \ 2\frac{1+r}{1-s} - 1 \\[2mm] b & = \quad s \end{cases}$$

and

$$\hat{R} \quad \longrightarrow \qquad\qquad \hat{T}$$

$$\mathcal{F}_{\hat{R}/\hat{T}} \quad :$$

$$(a\,,b) \quad \longrightarrow \quad \begin{cases} r \;=\; \dfrac{(1+a)(1-b)}{2} - 1 \\[2ex] s \;=\; \qquad\quad b \end{cases}$$

Finally, the basis functions $\{g_{lm}\}_{(l,m)\in S}$ with

$S = \{l \ge 0,\; m \ge 0,\; l \le L,\; l+m \le M,\; L \le M\}$ are defined by

$$g_{lm} \;=\; P_l^{0,0}(a)\,(1-b)^l\, P_m^{2l+1,0}(b)$$

where $P_n^{\alpha,\beta}(x)$ is the nth order Jacobi polynomial.

This basis is orthogonal and hierarchical. Besides, by evaluating the basis functions on the quadrilateral element, the volume integrals can be degenerated into the product of two one-dimensionnal integrations and then efficiently evaluated.

## 3.2.   Limiter for a $P^1$ (second order) approximation

Let's start with the case of the linear approximation to describe the limiting procedure. The Cockburn and Shu limiter is first reviewed.

The mean value of $\mathbf{U}_h$ on the triangle $K_0$ is denoted

$$\overline{\mathbf{U}}_T = \frac{1}{|T|} \int_T \mathbf{U}_h(\mathbf{x})\; d\mathbf{x} \tag{31}$$

For the set of Dubiner basis functions, it is reduced to $\overline{\mathbf{U}}_T = \mathbf{U}_{1,T}$.

We introduce

$$\widetilde{\mathbf{U}}_h(\mathbf{x}) = \sum_{i=1}^{3} \mathbf{U}_i(t)\Phi_i(\mathbf{x}) - \overline{\mathbf{U}}_T \qquad (32)$$

Given a triangle $K_0$, its neighbours are denoted by $K_1, K_2$, and $K_3$, and the middles of the edge $j$ by $m_j$ -see Figure 7-.

The purpose is to restrict $\widetilde{\mathbf{U}}_h$ in order to have $\mathbf{U}_h(x) \in [a,\ b]$ where $a = \min\{\overline{U}_{K_0}, \overline{U}_{K_1}, \overline{U}_{K_2}, \overline{U}_{K_3}\}$ and $b = \max\{\overline{U}_{K_0}, \overline{U}_{K_1}, \overline{U}_{K_2}, \overline{U}_{K_3}\}$.

The method consists in limiting $\widetilde{\mathbf{U}}_h$ on the middles of the edges of $K_0$. It comes to determine $\widetilde{\mathbf{U}}_1$, $\widetilde{\mathbf{U}}_2$ and $\widetilde{\mathbf{U}}_3$ on $K_0$ such that

$$\widetilde{\mathbf{U}}_h(\mathbf{x}) = \sum_{i=1}^{3} \widetilde{\mathbf{U}}_i(t)\Phi_i(\mathbf{x}) \qquad (33)$$

The modified quantities $\widetilde{\mathbf{U}}_h(m_i)$ for $i = 1, 2, 3$ are denoted by $\Delta_i$.

Finally, one gets on triangle $K_0$ :

$$\Lambda\Pi_h\mathbf{U}_h = \left(\mathbf{U}_1 + \widetilde{\mathbf{U}}_1\right)\Phi_1 + \widetilde{\mathbf{U}}_2\Phi_2 + \widetilde{\mathbf{U}}_3\Phi_3 \qquad (34)$$

with

$$\begin{cases} \widetilde{\mathbf{U}}_1 &= \frac{1}{3}(\Delta_1 + \Delta_2 + \Delta_3) \\[2mm] \widetilde{\mathbf{U}}_2 &= \frac{-1}{3}(2\Delta_1 - \Delta_2 - \Delta_3) \\[2mm] \widetilde{\mathbf{U}}_3 &= \frac{1}{2}(\Delta_2 - \Delta_3) \end{cases} \qquad (35)$$

Necessarily, in order to preserve the mean value of $\mathbf{U}_h$ on $K_0$, we must have $\widetilde{\mathbf{U}}_1 = 0$. Otherwise, a modification on $\Delta_i$ is performed to maintain the conservation of mass element by element (see [17] for more details).

The calculation of the quantities $\Delta_i$ is based on a geometrical property, namely the existence of non-negative coefficients $\alpha_i$ and $\beta_i$, $i = 1, 2, 3$ such that

$$
\begin{aligned}
m_1 - B_0 &= \alpha_1 (B_1 - B_0) + \beta_1 (B_2 - B_0) \\
m_2 - B_0 &= \alpha_2 (B_2 - B_0) + \beta_2 (B_3 - B_0) \\
m_3 - B_0 &= \alpha_3 (B_3 - B_0) + \beta_3 (B_1 - B_0)
\end{aligned}
\tag{36}
$$

Quantities $\Delta_i$ are defined in the following way :

$$
\begin{aligned}
\Delta_1 &= \operatorname{minmod}\left(\mathbf{U}_h(m_1) - \overline{\mathbf{U}}_{K_0}, \nu\left(\alpha_1\left(\overline{\mathbf{U}}_{K_1} - \overline{\mathbf{U}}_{K_0}\right) + \beta_1\left(\overline{\mathbf{U}}_{K_2} - \overline{\mathbf{U}}_{K_0}\right)\right)\right) \\
\Delta_2 &= \operatorname{minmod}\left(\mathbf{U}_h(m_2) - \overline{\mathbf{U}}_{K_0}, \nu\left(\alpha_2\left(\overline{\mathbf{U}}_{K_2} - \overline{\mathbf{U}}_{K_0}\right) + \beta_2\left(\overline{\mathbf{U}}_{K_3} - \overline{\mathbf{U}}_{K_0}\right)\right)\right) \\
\Delta_3 &= \operatorname{minmod}\left(\mathbf{U}_h(m_3) - \overline{\mathbf{U}}_{K_0}, \nu\left(\alpha_3\left(\overline{\mathbf{U}}_{K_3} - \overline{\mathbf{U}}_{K_0}\right) + \beta_3\left(\overline{\mathbf{U}}_{K_1} - \overline{\mathbf{U}}_{K_0}\right)\right)\right)
\end{aligned}
\tag{37}
$$

where $\nu > 1$.

Now, the objective is to get a less diffusive method. For a given point P on interface j, $\mathbf{U}_h^-(P)$ is refered to the approximation of $\mathbf{U}(P)$ issued from triangle $K_0$, and $\mathbf{U}_h^+(P)$ the approximation issued from $K_j$.

The following method -which brings in a very simple procedure- improves a lot numerical results. We define

$$\Delta_{j,m} =$$

$$\text{minmod}\left(\mathbf{U}_h^-(m_j) - \overline{\mathbf{U}}_{K_0}, \nu\left(\alpha_j\left(\overline{\mathbf{U}}_{K_1'} - \overline{\mathbf{U}}_{K_0}\right) + \beta_j\left(\overline{\mathbf{U}}_{K_2'} - \overline{\mathbf{U}}_{K_0}\right)\right)\right) \qquad (38)$$

"Large" gradients are identified by $\Delta_{j,m} \neq \mathbf{U}_h^-(m_j) - \overline{\mathbf{U}}_{K_0}$. If the equality is satisfied then the quantity $\mathbf{U}_h^-(m_j) - \overline{\mathbf{U}}_{K_0}$ is preserved. Otherwise, the maxmod function is introduced to relax the minmod function effects according to the approximate solution regularity. We introduce

$$\Delta_{j,max} = \text{minmod}\left(\mathbf{U}_h^-(m_j) - \overline{\mathbf{U}}_{K_0}, \mathbf{U}_h^+(m_j) - \overline{\mathbf{U}}_{K_0}\right) \qquad (39)$$

Limited gradients are defined by

$$\Delta_j = \text{maxmod}\left(\Delta_{j,m}, \Delta_{j,max}\right) \qquad (40)$$

### 3.3.  Limiter for a $P^2$ (third order) approximation

As shown for one-dimensional problems, the differentiation process allows the adaptation of the slope limiter to any order of polynomial approximations. Given the good numerical results obtained in 1D, the method is generalized to $P^2$ case by making use of the same methodology.

A question which arises from the elaboration of the technique for triangular meshes is concerned with the direction of derivatives and quantities to be limited. Two methods can be used : firstly, derivatives in the flow direction can be computed and limited, in order to derive a totally multi-dimensional proceeding. This feasibility has been ruled out since the way of establishing a well defined method is

not clear. Secondly, one way consists in differentiating along the vector joining the center of gravity of each triangle to the middles of its edges. It leads to a scheme which depends on the mesh geometry (as for the Cockburn and Shu method) which is presented in what follows.

Given $\mathbf{n}_i = \dfrac{\overrightarrow{B_0 m_i}}{\left|\overrightarrow{B_0 m_i}\right|}$ $(i = 1, 2, 3)$ normalized vectors on triangle $K_0$. The quantities to be limited are

$$\mathbf{W}_{h,\mathbf{n}_i} = \frac{\partial \mathbf{U}_h}{\partial \mathbf{n}_i}^-(m_i) - \frac{\partial \mathbf{U}_h}{\partial \mathbf{n}_i}(B_0) \tag{41}$$

The affected triangle is not precised when there is no ambiguity. Vectors $\mathbf{n}_i$ are computed in reference to triangle $K_0$. Moreover, as jumps are permitted at interfaces of elements, there are two different values for the approximate solution on each edge of the triangles. Symbol $-$ is related to values on $K_0$ and symbol $+$ to values on one of its neighbours.

Now, the method can be fully defined. Let us define :

$$\mathbf{Z}_{h,\mathbf{n}_i} = \alpha_i \left( \frac{\partial \mathbf{U}_h}{\partial \mathbf{n}_i}(B_1') - \frac{\partial \mathbf{U}_h}{\partial \mathbf{n}_i}(B_0) \right) + \beta_i \left( \frac{\partial \mathbf{U}_h}{\partial \mathbf{n}_i}(B_2') - \frac{\partial \mathbf{U}_h}{\partial \mathbf{n}_i}(B_0) \right) \tag{42}$$

We set

$$\Delta 2_{\mathbf{n}_i,m} = \mathrm{minmod}\left(W_{h,\mathbf{n}_i}, \nu \mathbf{Z}_{h,\mathbf{n}_i}\right) \tag{43}$$

and

$$\Delta 2_{\mathbf{n}_i, max} = \text{minmod}\left(W_{h,\mathbf{n}_i}, \frac{\partial \mathbf{U}_h}{\partial \mathbf{n}_i}^{+}(m_i) - \frac{\partial \mathbf{U}_h}{\partial \mathbf{n}_i}(B_0)\right) \tag{44}$$

Finally, if $\Delta 2_{\mathbf{n}_i, m} \neq W_{h,\mathbf{n}_i}$ then $\Delta 2_{\mathbf{n}_i} = \text{maxmod}\left(\Delta 2_{\mathbf{n}_i, m}, \Delta 2_{\mathbf{n}_i, max}\right)$ takes the place of $W_{h,\mathbf{n}_i}$ (for $i = 1, 2, 3$).

Contrary to the one-dimensionnal case, the change from $P^1$ to $P^2$ basis adds three degrees of freedom. To overcome this difficulty, degrees of freedom $\widetilde{U}_4$, $\widetilde{U}_5$ and $\widetilde{U}_6$ are computed by freezing the moments $U_1$, $U_2$ and $U_3$ (moments $\widetilde{U}_1$, $\widetilde{U}_2$ and $\widetilde{U}_3$ are computed with the method elaborated for linear approximations). In brief, on triangle $K_0$ we come down to the system to be inversed

$$\begin{cases} \dfrac{\partial \mathbf{U}_h}{\partial \mathbf{n}_1}(m_1) - \dfrac{\partial \mathbf{U}_h}{\partial \mathbf{n}_1}(B_0) = G_1\left(\mathbf{U}_{1,K_0}, \mathbf{U}_{2,K_0}, \mathbf{U}_{3,K_0}\right) + \displaystyle\sum_{i=4}^{6} \gamma_i \widetilde{\mathbf{U}}_{i,K_0} \\[2mm] \dfrac{\partial \mathbf{U}_h}{\partial \mathbf{n}_2}(m_2) - \dfrac{\partial \mathbf{U}_h}{\partial \mathbf{n}_2}(B_0) = G_2\left(\mathbf{U}_{1,K_0}, \mathbf{U}_{2,K_0}, \mathbf{U}_{3,K_0}\right) + \displaystyle\sum_{i=4}^{6} \xi_i \widetilde{\mathbf{U}}_{i,K_0} \\[2mm] \dfrac{\partial \mathbf{U}_h}{\partial \mathbf{n}_3}(m_3) - \dfrac{\partial \mathbf{U}_h}{\partial \mathbf{n}_3}(B_0) = G_3\left(\mathbf{U}_{1,K_0}, \mathbf{U}_{2,K_0}, \mathbf{U}_{3,K_0}\right) + \displaystyle\sum_{i=4}^{6} \mu_i \widetilde{\mathbf{U}}_{i,K_0} \end{cases} \tag{45}$$

with

$$\begin{aligned} G_j &= \sum_{i=1}^{3} \widetilde{\mathbf{U}}_{i,K_0}\left(\frac{\partial \phi_i}{\partial \mathbf{n}_j}(m_j) - \frac{\partial \phi_i}{\partial \mathbf{n}_j}(B_0)\right) & j &= 1, 2, 3 \\[2mm] \gamma_i &= \frac{\partial \phi_i}{\partial \mathbf{n}_1}(m_1) - \frac{\partial \phi_i}{\partial \mathbf{n}_1}(B_0) & i &= 1, 2, 3 \\[2mm] \xi_i &= \frac{\partial \phi_i}{\partial \mathbf{n}_2}(m_2) - \frac{\partial \phi_i}{\partial \mathbf{n}_2}(B_0) & i &= 1, 2, 3 \\[2mm] \mu_i &= \frac{\partial \phi_i}{\partial \mathbf{n}_3}(m_3) - \frac{\partial \phi_i}{\partial \mathbf{n}_3}(B_0) & i &= 1, 2, 3 \end{aligned} \tag{46}$$

The regularity criterion of the solution is based on terms $\mathbf{U}_4$, $\mathbf{U}_5$ and $\mathbf{U}_6$. In practice, the following test is used :

1. If $\widetilde{\mathbf{U}}_4 = \mathbf{U}_4$, $\widetilde{\mathbf{U}}_5 = \mathbf{U}_5$ and $\widetilde{\mathbf{U}}_6 = \mathbf{U}_6$ then limiter's effects on the linear part of the approximation are suppressed :

$$\widetilde{\mathbf{U}}_1 = \mathbf{U}_1, \ \widetilde{\mathbf{U}}_2 = \mathbf{U}_2, \ \widetilde{\mathbf{U}}_3 = \mathbf{U}_3$$

Else,

2. all the degrees of freedom of $\mathbf{U}_h$ are limited.

By this process, as for the one-dimensional case, the limiting procedure is generalizable to $P^k$ approximations. One only has to differentiate the approximate solution several times, to get a linear term which can then be limited with the method based on $P^1$ approximations.

### 3.4.   Boundary conditions

The main difficulty is to impose the slip condition on the walls in a stable way. As mentionned in [3], the inviscid interface integral terms are constructed with a technique traditionally used in upwind Finite Volume schemes. The flux function $F(\mathbf{U}) \cdot \mathbf{n}$ is replaced by a numerical flux function $h(\mathbf{U}^-, \mathbf{U}_{bc}; \mathbf{n})$, depending on the internal interface state $\mathbf{U}^-$ and the boundary condition $\mathbf{U}_{bc}$. At solid walls, the flux function $F(\mathbf{U}) \cdot \mathbf{n}$ is equal to the pressure contribution in the direction normal to the wall. The pressure is taken from the internal boundary state.

Besides, a special treatment is necessary for the limiting procedure. Indeed, to limit the gradients of the approximate solution on the sides of a triangle $K_0$, the method makes use of the three neighboors $K_1$, $K_2$ and $K_3$. The formulation for a solid wall boundary condition is presented in what follows.

Given a triangle $K_0$ on the domain boundary, its edges are denoted by $e_j$, $(j = 1, 2, 3)$ with $e_1 \cap \partial\Omega \neq \emptyset$ and $e_j \cap \partial\Omega = \emptyset$ for $j = 2, 3$.

For the limiting procedure, boundary conditions are imposed by providing a complete solution on the dummy cell $K_0'$ (see Figure 9). The exterior solution is reconstructed from the interior one by considering the Gauss points used to evaluate the volume integrals. Let $M$ be a Gauss point on triangle $K_0$, $M'$ its symmetric on $K_0'$. A symmetry technique is used point by point whereby the state $\mathbf{U}_h(M')$ on cell $K_0'$ has the same density, internal energy and tangential velocity component of $\mathbf{U}_h(M)$ and the opposite sign normal velocity component.

In order to increase the stability, the limiting procedure is slightly modified to involve a vector normal to the boundary, as in Bruneau and Rasetarinera [8]. For a linear approximation, the gradients of $\mathbf{U}_h$ are then limited on the midles $m_2$ and $m_3$ of the edges $e_2$ and $e_3$, and on the orthogonal projection of the center of gravity of the triangle $K_0$ on the boundary edge $e_3$.

For a third-order approximation, the quantity to be limited related to the boundary edge is :

$$\frac{\partial \mathbf{U}_h}{\partial \mathbf{n}}(H) - \frac{\partial \mathbf{U}_h}{\partial \mathbf{n}}(B_0)$$

with $\mathbf{n} = \overrightarrow{B_0 H}$.

## 3.5.  Numerical results

### 3.5.1.  Shu and Osher test case

This test case is reconsidered with the two-dimensional slope limiter to show the procedure elaborated for the one-dimensional case has been well extended to triangular meshes. Numerical results exhibit an improved solution with $P^2$ approximation (see Figure 10 for comparison). The proposed algorithm for unstructured meshes leads to bounded solutions near discontinuities. Besides, a $P^2$ truncated solution is shown on Figure 11. In practice, the approximate solution has been locally reduced to a linear term in the vicinity of shocks. Extrema of the resulting solution are more flattened that those of the not-truncated solution. Finally, Figure 11 shows the improvement due to the regularity criterion previously described. So, the whole procedure is needed.

Some test results about accuracy are now given for the second and the third order limited schemes.

### 3.5.2. Accuracy test

The first example is the two dimensional linear equation $u_t + u_x + u_y = 0$ with the initial condition $u_0(x, y) = \sin(\pi(x + y))$ $(-1 \leq x, y \leq 1)$ and periodic boundary conditions. Uniform triangular meshes are first considered. Issued from a uniform cartesian mesh, they are obtained by adding one diagonal line in each rectangle. The coarsest one is shown in Figure 12. It corresponds to $h = h_0 = 1/2$ where h is the length of the rectangles. The results at time t=2 are shown in Table V.

Non-uniform meshes are next considered. The coarsest mesh is shown in Figure 13. A serie of meshes is obtained by refining the mesh in a uniform way (each triangle is divided into four smaller ones). The results are presented in Table VI.

The same equation is reconsidered with the initial condition $u_0(x, y) = \sin^4(\pi(x + y))$ and the same meshes -see Tables VII and VIII-. As for the one-dimensional case, a loss of accuracy takes place in the $L^\infty$-norm but not in the $L^1$-norm.

The accuracy of the method for nonlinear problems is illustrated with the system of Euler equations. This test case is proposed by Shu in [23]. The initial condition is obtained by adding an isentropic vortex to a mean flow ($\rho_0 = 1$, $u_0 = 1$, $v_0 = 1$, $p_0 = 1$). The vortex is a perturbation to the velocity $(u, v)$, the temperature $T$, the entropy $S$ and is denoted by the tilde values :

$$
\begin{aligned}
\tilde{u} &= \tfrac{\epsilon}{2\pi} e^{0.5(1-r^2)} (5 - y) \\
\tilde{v} &= \tfrac{\epsilon}{2\pi} e^{0.5(1-r^2)} (x - 5) \\
\tilde{T} &= -\tfrac{(\gamma-1)\epsilon^2}{8\gamma\pi^2} e^{1-r^2} \\
\tilde{S} &= 0
\end{aligned}
$$

with $\epsilon = 5$, $r = \sqrt{(x - 5)^2 + (y - 5)^2}$.

An analytic solution of the problem is known. The computational domain is taken as $[0, 10] \times [0, 10]$ with periodic boundary conditions in both directions. Error are shown at time t=2 for uniform and nonuniform meshes (same kind of meshes as for the previous example) in Tables IX and X. The rate of convergence is preserved in the $L^1$-norm.

Three bidimensional problems are now presented to illustrate the capacity of the new limiter to capture strong gradients, whatever the order of accuracy of the

approximate solution (two or three for the present paper). It is important to notice that only unstructured nonuniform triangular meshes are considered.

### 3.5.3. Reflection of a plane shock from a ramp

This problem was studied in Quirk [29] and Abgrall [1]. A planar shock initially enters from the left in a quiescent fluid and is reflected from a 45 degrees ramp. The Mach number is $M_s = 5.5$ and the undisturbed air ahead of the shock has a density of 1.4 and a pressure of 1. Reflecting boundary conditions are applied along the ramp and the bottom and the upper of the problem domain. Values for the initial flow are assigned at the left and right-hand boundaries. The simulation is performed with second-order approximate solutions. Results obtained with the Biswas et al. limiter and the new method are compared in what follows.

For such an incident shock wave Mach number and such a reflecting wedge angle, a double Mach reflection is expected (further details about shock wave phenomena can be found in [5]) . For a linear approximation, the slipstream coming from the Mach stem is better resolved with the new limiter -see Figure 14-.

### 3.5.4. Step marching problem

It concerns a flow past a forward-facing step. This test case has been extensively studied by Woodward and Colella [41], and is widely present in the literature (for comparison, see for example [8], [17]). The problem starts with uniform Mach 3 flow in a wind tunnel containing a step. The wind tunnel is 1 length unit wide and 3 length units long. The step is 0.2 length units high and is located at 0.6 length units from the inflow plane. Reflecting boundary conditions are applied along the walls of the tunnel, and inflow and outflow boundary conditions are applied at the

entrance and the exit of the tunnel.

The corner of the step is a singularity. It is well known that if no special treatment is done, an entropy production is observed in the vicinity of the step corner, and it alters the quality of the second reflected shock. However, neither artefacts to impose the slip condition at the corner, nor positivity correction procedure have been employed.

The value of the CFL number is 0.3 for the $P^1$ and 0.18 for the $P^2$ approximations. Two unstructured meshes have been considered. The first one (mesh A) contains 13774 triangles. It is locally refined near the corner. The second mesh (mesh B) contains 14392 elements. Details of the meshes around the corner are shown in the Figure 15.

The erroneous entropy production near the corner induces a numerical boundary layer visible on the density contours, and especially on the Mach number and the entropy function contours.

Results are shown in Figures 16 to 22. The entropy layer at the downstream bottom wall is clearly reduced by the $P^2$ approximation, and by a local refinement of the mesh near the singularity. The reflected shock on the lower part of the step is improved with the higher-order method. Second-order results obtained with the minmod limiter are shown on Figure 19. The maxmod function clearly improves the contact discontinuity.

*3.5.5.  Shock passing a backward facing corner*

This last test case is presented to demonstrate the ability of the new method to evaluate strong gradients. The computational domain is $\Omega = ([0,1] \times [6,11]) \cup ([1,13] \times [0,11])$. A right-moving shock of $M_s = 5.09$ is initially located at $x = 0.5$. The undisturbed air ahead of the shock has a density of 1.4 and a pressure of 1. Inflow and outflow boundary conditions are respectively applied at $x = 0$ and $x = 13$. The boundary conditions are reflective everywhere else.

The simulation is performed with the $P^2$-version of the limiter, for two different meshes (which contain respectively 8464 and 23638 elements) -see results on Figure 23-. Contrary to [17], no positivity correction procedure is needed to avoid negative density or pressure. Besides, the scheme is not modified at the corner of the step, which is a singularity of the problem. The limiting procedure is then well adapted to strong shocks even with unstructured meshes.

## 4.  CONCLUSION

In this paper, a new slope limiter to treat solutions with discontinuities with RKDG method of arbitrary order of accuracy has been presented. The method has been first described for one-dimensional problems. Numerical results point out that the proposed stabilization procedure does not degrade the accuracy of the method at smooth extrema in the $L^1$-norm. Furthermore, solutions with discontinuities are well captured, without spurious oscillations, whathever the order of accuracy of the method is. At last, the resulting numerical approximation is better as the degree of the polynomial expansion increases.

Next, the new method has been extended to the case of two-dimensional unstructured triangular meshes, for $P^1$ and $P^2$ approximations. It has been noticed that the procedure is generalizable to any order of accuracy.

The paper developed extensive details concerning two points, the definition of a regularity criterion to determine regions where the solution needs to be stabilized, and a way of limiting without introducing too much numerical viscosity. This is done without any dependence of the procedure to the considered problem. That is the main first advantage of the proposed scheme, the second one being the capacity of the method to handle unstructured triangular meshes.

# REFERENCES

1. R. Abgrall. On essentially non-oscillatory schemes on unstructured meshes : Analysis and implementation. *J. Comput. Phys.*, **114**:45–58, (1994).

2. H.L. Atkins and C.-W. Shu. Quadrature-Free Implementation of Discontinuous Galerkin Method for Hyperbolic Equations. *Technical Report 96-51, ICASE report*, (1996).

3. F. Bassi and S. Rebay. A High-Order Accurate Discontinuous Finite Element Method for the Numerical Solution of the Compressible Navier-Stokes Equations. *J. Comput. Phys.*, **131**:267–279, (1997).

4. F. Bassi and S. Rebay. An Implicit High-Order Discontinuous Galerkin Method for the Steady State Compressible Navier-Stokes Equations. *ECCOMAS*, (1998).

5. G. Ben-Dor. *Shock wave reflection phenomena.* (Springer-Verlag, 1991).

6. R. Biswas, K. D. Devine, and J.E. Flaherty. Parallel, adaptive finite element methods for conservation laws. *Appl. Numer. Math.*, **14**:255–283, (1994).

7. M. Borrel and B. Berde. Moment approach for the Navier-Stokes equations. AIAA paper 95-1663, (1995).

8. Ch.-H. Bruneau and P. Rasetarinera. A Finite Volume Method With Efficient Limiters For Solving Conservation Laws. *CFD J.*, **6**:1, (1997).

9. G. Chavent and B. Cockburn. The Local projection $P^0 P^1$ Discontinuous Galerkin Finite Element Method For Scalar Conservation Laws. *$M^2 AN$*, **23**:565–592, (1989).

10. G. Chavent and G. Salzano. A Finite Element Method for the 1D water flooding problem with gravity. *J. Comput. Phys.*, **45**:307–344, (1982).

11. B. Cockburn. Discontinuous Galerkin Methods for Convection-Dominated Problems. In T.J. Barth and H. Deconinck, editors, *High-Order Methods for Computational Physics*, volume 9 of *Lecture Notes in Computational Science and Engineering*, pages 69–224. Springer, (1999).

12. B. Cockburn and C.-W. Shu. TVB Runge-Kutta Local Projection Discontinuous Galerkin Finite Element Method for Conservation Laws II: General Framework. *Math. Comput.*, **52**(186):411–435, (1989).

13. B. Cockburn and C.-W. Shu. TVB Runge-Kutta Local Projection Discontinuous Galerkin Finite Element Method for Conservation Laws III: One-Dimensional Systems. *J. Comput. Phys.*, **84**:90–113, (1989).

14. B. Cockburn and C.-W. Shu. The Runge-Kutta Local Projection Discontinuous Galerkin Finite Element Method for Conservation Laws IV: The multidimensional case. *Math. Comput.*, **54**(190):545–581, (1990).

15. B. Cockburn and C.-W. Shu. The Runge-Kutta Local Projection $P^1$-Discontinuous-Galerkin Finite Element Method for Scalar Conservation Laws. $M^2AN$, **25**:337–361, (1991).

16. B. Cockburn and C.-W. Shu. The Local Discontinuous Galerkin Method for Time-Dependent Convection-Diffusion Systems. *J. Numer. Anal.*, **35**:2440–2463, (1998).

17. B. Cockburn and C.-W. Shu. The Runge-Kutta Discontinuous Galerkin Method for Conservation Laws V : Multidimensional Systems. *J. Comput. Phys.*, **141**:199–224, (1998).

18. K. D. Devine and J.E. Flaherty. Parallel adaptive hp-refinement techniques for conservation laws. *Appl. Numer. Math.*, **20**:367–386, (1996).

19. C. Drozo, M. Borrel, and A. Lerat. Un schéma de type Galerkin Discontinu pour les systèmes hyperboliques. 29$^{\text{ème}}$ Congrès Français d'Analyse Numérique, Larnas, Mai 1997.

20. C. Drozo, M. Borrel, and A. Lerat. Discontinuous Galerkin schemes for the compressible Navier-Stokes equations. In *Lecture Notes in Physics*, 16th Int. Conf. on Numer. Methods in Fluid Dynamics. Arcachon (France), pages 266–272. Springer, (1998).

21. M. Dubiner. Spectral Methods on Triangles and Other Domains. *J. Sci. Comput.*, 6(4), (1991).

22. A. Harten, B. Engquist, S. Osher, and S. R. Chakravarthy. Uniformly high-order accurate essentially nonoscillatory schemes. *J. Comput. Phys.*, **71**:231, (1987).

23. Changqing Hu and Chi-Wang Shu. Weighted Essentially Non-oscillatory Schemes on Triangular Meshes. *J. Comput. Phys.*, **150**:97–127, (1999).

24. N. Huré, C. Drozo, and M. Borrel. Une méthode multigrille pour un schéma de type Galerkin discontinu. 30$^{\text{ème}}$ Congrès Français d'Analyse Numérique, Arles, Mai 1998.

25. G. Jiang and C.-W. Shu. On Cell Entropy Inequality for Discontinuous Galerkin Methods. *ICASE report 93-37*, (1997).

26. P. Lesaint and P.A. Raviart. *On a Finite Element method to solve the neutron transport equation.* Partial Differentiel Equations. C. de Boor, Academic Press, New York edition, (1974).

27. S.Y. Lin, Y.S. Chin, Y.F. Dung, C.C. Hong, Y.Y. Wang, and C.H. Ko. Discontinuous Galerkin Finite Element Method for Two Dimensional Conservation Laws. 31st Aerospace Sciences meeting and Exhibit. AIAA paper 93-0337, (1987).

28. I. Lomtev, C.B. Quillen, and G.E. Karniadakis. Spectral /hp Methods for Viscous Compressible Flows on Unstructured 2d meshes. *J. Comput. Phys.*, **144**:325–357, (1998).

29. James J. Quirk. A Contribution to The Great Riemann Solver Debate. *ICASE report 92-64*, (1992).

30. W.H. Reed and T.R. Hill. Triangular mesh methods for the neutron transport equation. *Technical Report LA-UR-73-479*, (1973).

31. Denis Serre. *Systèmes de Lois de conservation I.* (Diderot Editeur, Fondations), (1996).

32. S.J. Sherwin and G.E. Karniadakis. A new triangular and tetrahedral basis for high-order (hp) finite element methods. *Int. J. for Numer. Meth. in Eng.*, **38**:3775–3802, (1995).

33. S.J. Sherwin and G.E. Karniadakis. A Triangular Spectral Element Method; applications to the incompressible Navier-Stokes equations. *Comput. Methods Appl. Mech. Engrg.*, **123**:189–229, (1995).

34. S.J. Sherwin and G.E. Karniadakis. Tetrahedral hp Finite Elements: Algorithms and Flows Simulations. *J. Comput. Phys.*, **124**:14–45, (1996).

35. C.-W. Shu. TVB Uniformly High-Order Schemes for Conservation Laws. *Math. Comput.*, **49**:105–121, (1987).

36. C.-W. Shu. Total-Variation-Diminishing time discretizations. *SIAM J. Sci. Stat. Comput.*, **9**:1073–1084, (1988).

37. C.-W. Shu and S. Osher. Efficient implementation of essentially non-oscillatory shock capturing schemes II. *J. Comput. Phys.*, **83**:32–78, (1989).

38. A. Suresh and H. T. Huynh. Accurate Monotonicity-Preserving Schemes with Runge-Kutta Time Stepping. *J. Comput. Phys.*, **136**:83–99, (1997).

39. B. Van Leer. Towards the Ultimate Conservative Difference Scheme. V.A Second-Order Sequel to Godunov's Method. *J. Comput. Phys.*, **32**:101–136, (1979).

40. Monika Wierse. A new theoretically motivated higher order upwind scheme on unstructured grids of simplices. *Adv. Comput. Math.*, **7**:303–335, (1997).

41. P. Woodward and P. Colella. The numerical simulation of two-dimensional fluid flow with strong shocks. *J. Comput. Phys.*, **54**:115–173, (1984).

**TABLE I**

**Accuracy for 1D Transport equation, $u_0(x) = sin(\pi x)$**

|  | $\Delta x$ | $P^1$ (second order) | | $P^2$ (third order) | | $P^3$ (fourth order) | |
|---|---|---|---|---|---|---|---|
|  |  | $L^1$-error | order | $L^1$-error | order | $L^1$-error | order |
| unlimited | 1/16 | 2.60E-03 | - | 2.88E-05 | - | 3.31E-07 | - |
|  | 1/32 | 6.49E-04 | 2.00 | 3.60E-06 | 3.00 | 2.07E-08 | 4.00 |
|  | 1/64 | 1.62E-04 | 2.00 | 4.50E-07 | 3.00 | 1.29E-09 | 4.00 |
|  | 1/128 | 4.05E-05 | 2.00 | 5.62 E-08 | 3.00 | 8.09E-11 | 4.00 |
|  | 1/256 | 1.06E-05 | 2.00 | 7.03E-09 | 3.00 | 5.20E-12 | 3.95 |
| DG$^{\mathrm{min}}$ | 1/16 | 1.35E-02 | - | 2.68E-04 | - | 3.32E-06 | - |
|  | 1/32 | 2.83E-03 | 2.25 | 2.88E-05 | 3.21 | 1.72E-07 | 4.26 |
|  | 1/64 | 5.86E-04 | 2.27 | 2.95 E-06 | 3.29 | 9.17E-09 | 4.23 |
|  | 1/128 | 1.21E-04 | 2.26 | 3.00E-07 | 3.29 | 4.79E-10 | 4.25 |
|  | 1/256 | 2.57E-05 | 2.24 | 3.03 E-08 | 3.30 | 2.56E-11 | 4.22 |
| DG$^{\mathrm{max}}$ | 1/16 | 1.10E-02 | - | 2.13E-04 | - | 1.43E-06 | - |
|  | 1/32 | 2.36E-03 | 2.23 | 2.41E-05 | 3.14 | 1.08E-07 | 3.72 |
|  | 1/64 | 4.86E-04 | 2.28 | 2.61E-06 | 3.20 | 7.26E-09 | 3.89 |
|  | 1/128 | 1.02E-04 | 2.25 | 2.79E-07 | 3.22 | 4.30E-10 | 4.07 |
|  | 1/256 | 2.18E-05 | 2.22 | 2.93E-08 | 3.25 | 2.44E-11 | 4.14 |

**TABLE II**

**Accuracy for 1D Transport equation, $u_0(x) = sin(\pi x)$**

|  | $\Delta x$ | $P^1$ (second order) | | $P^2$ (third order) | | $P^3$ (fourth order) | |
|---|---|---|---|---|---|---|---|
|  |  | $L^\infty$-error | order | $L^\infty$-error | order | $L^\infty$-error | order |
| unlimited | 1/16 | 2.85E-03 | - | 3.22E-05 | - | 4.62E-07 | - |
|  | 1/32 | 6.81E-04 | 2.06 | 4.03E-06 | 3.00 | 2.89E-08 | 3.99 |
|  | 1/64 | 1.66E-04 | 2.03 | 5.04E-07 | 3.00 | 1.81E-09 | 3.99 |
|  | 1/128 | 4.10E-05 | 2.02 | 6.29E-08 | 3.00 | 1.13E-10 | 3.99 |
|  | 1/256 | 1.02E-05 | 2.01 | 7.86E-09 | 3.00 | 7.96E-12 | 3.83 |
| DG$^{min}$ | 1/16 | 3.17E-02 | - | 8.75E-04 | - | 1.43E-05 | - |
|  | 1/32 | 1.05E-02 | 1.59 | 1.64E-04 | 2.41 | 1.31E-06 | 3.44 |
|  | 1/64 | 3.47E-03 | 1.60 | 2.92E-05 | 2.49 | 1.21E-07 | 3.44 |
|  | 1/128 | 1.13E-03 | 1.61 | 5.10E-06 | 2.51 | 1.10E-08 | 3.45 |
|  | 1/256 | 3.68E-04 | 1.62 | 8.88E-07 | 2.52 | 1.00E-09 | 3.46 |
| DG$^{max}$ | 1/16 | 2.75E-02 | - | 8.01E-04 | - | 6.31E-06 | - |
|  | 1/32 | 1.04E-02 | 1.39 | 1.50E-04 | 2.42 | 7.91E-07 | 2.99 |
|  | 1/64 | 3.17E-03 | 1.72 | 2.74E-05 | 2.45 | 9.78E-08 | 3.01 |
|  | 1/128 | 8.97E-04 | 1.82 | 4.97E-06 | 2.46 | 1.00E-08 | 3.28 |
|  | 1/256 | 2.95E-04 | 1.60 | 8.8E-07 | 2.49 | 9.59E-10 | 3.39 |

**TABLE III**

Accuracy for 1D Transport equation, $u_0(x) = sin^4(\pi x)$

| | $\Delta x$ | $P^1$ (second order) | | $P^2$ (third order) | | $P^3$ (fourth order) | |
|---|---|---|---|---|---|---|---|
| | | $L^1$-error | order | $L^1$-error | order | $L^1$-error | order |
| unlimited | 1/16 | 0.18E-01 | - | 0.43E-03 | - | 0.18E-04 | - |
| | 1/32 | 0.26E-02 | 2.75 | 0.51E-04 | 3.03 | 0.11E-05 | 4.00 |
| | 1/64 | 0.55E-03 | 2.25 | 0.64E-05 | 2.99 | 0.71E-07 | 4.00 |
| | 1/128 | 0.13E-03 | 2.06 | 0.79E-06 | 3.00 | 0.45E-08 | 4.00 |
| | 1/256 | 0.32E-04 | 2.02 | 0.99E-07 | 3.00 | 0.28E-09 | 4.00 |
| $DG^{min}$ | 1/16 | 0.81E-01 | - | 0.90E-02 | - | 0.19E-02 | - |
| | 1/32 | 0.17E-01 | 2.25 | 0.10E-02 | 3.12 | 0.74E-04 | 4.70 |
| | 1/64 | 0.34E-02 | 2.33 | 0.10E-03 | 3.31 | 0.31E-05 | 4.57 |
| | 1/128 | 0.66E-03 | 2.34 | 0.10E-04 | 3.33 | 0.13E-06 | 4.59 |
| | 1/256 | 0.13E-03 | 2.31 | 0.10E-05 | 3.33 | 0.57E-08 | 4.51 |
| $DG^{max}$ | 1/16 | 0.78E-01 | - | 0.77E-02 | - | 0.14E-02 | - |
| | 1/32 | 0.16E-01 | 2.24 | 0.95E-03 | 3.02 | 0.62E-04 | 4.49 |
| | 1/64 | 0.33E-02 | 2.33 | 0.10E-03 | 3.25 | 0.28E-05 | 4.46 |
| | 1/128 | 0.65E-03 | 2.34 | 0.10E-04 | 3.30 | 0.12E-06 | 4.53 |
| | 1/256 | 0.13E-03 | 2.31 | 0.10E-05 | 3.31 | 0.55E-08 | 4.48 |

**TABLE IV**

Accuracy for 1D Transport equation, $u_0(x) = sin^4(\pi x)$

| | $\Delta x$ | $P^1$ (second order) | | $P^2$ (third order) | | $P^3$ (fourth order) | |
|---|---|---|---|---|---|---|---|
| | | $L^\infty$-error | order | $L^\infty$-error | order | $L^\infty$-error | order |
| unlimited | 1/16 | 0.19E-01 | - | 0.35E-03 | - | 0.15E-04 | - |
| | 1/32 | 0.35E-02 | 2.47 | 0.43E-04 | 3.03 | 0.93E-06 | 3.98 |
| | 1/64 | 0.67E-03 | 2.37 | 0.54E-05 | 2.99 | 0.58E-07 | 3.99 |
| | 1/128 | 0.14E-03 | 2.24 | 0.68E-06 | 3.00 | 0.36E-08 | 4.00 |
| | 1/256 | 0.32E-04 | 2.14 | 0.84E-07 | 3.00 | 0.23E-09 | 3.99 |
| $DG^{min}$ | 1/16 | 0.12E+00 | - | 0.98E-02 | - | 0.25E-02 | - |
| | 1/32 | 0.42E-01 | 1.48 | 0.19E-02 | 2.39 | 0.19E-03 | 3.75 |
| | 1/64 | 0.14E-01 | 1.57 | 0.33E-03 | 2.48 | 0.12E-04 | 3.94 |
| | 1/128 | 0.46E-02 | 1.60 | 0.59E-04 | 2.50 | 0.77E-06 | 4.01 |
| | 1/256 | 0.15E-02 | 1.62 | 0.10E-04 | 2.52 | 0.48E-07 | 4.00 |
| $DG^{max}$ | 1/16 | 0.11E+00 | - | 0.82E-02 | - | 0.25E-02 | - |
| | 1/32 | 0.41E-01 | 1.47 | 0.18E-02 | 2.20 | 0.18E-03 | 3.77 |
| | 1/64 | 0.14E-01 | 1.56 | 0.32E-03 | 2.46 | 0.12E-04 | 3.90 |
| | 1/128 | 0.46E-02 | 1.60 | 0.58E-04 | 2.47 | 0.76E-06 | 4.01 |
| | 1/256 | 0.15E-02 | 1.62 | 0.10E-04 | 2.51 | 0.48E-07 | 4.00 |

**TABLE V**

Accuracy for $u_t + u_x + u_y = 0$, $u_0(x, y) = sin(\pi(x + y))$. Uniform meshes.

| Scheme | h | $L^1$-norm | | $L^\infty$-norm | |
|---|---|---|---|---|---|
| | | error | order | error | order |
| $P^1$-unlimited | $\frac{h_0}{2}$ | 0.31E-01 | - | 0.44E-01 | - |
| | $\frac{h_0}{4}$ | 0.60E-02 | 2.34 | 0.99E-02 | 2.14 |
| | $\frac{h_0}{8}$ | 0.13E-02 | 2.22 | 0.29E-02 | 1.79 |
| | $\frac{h_0}{16}$ | 0.30E-03 | 2.13 | 0.76E-03 | 1.91 |
| $P^2$-unlimited | $\frac{h_0}{2}$ | 0.11E-02 | - | 0.33E-02 | - |
| | $\frac{h_0}{4}$ | 0.13E-03 | 3.04 | 0.42E-03 | 2.99 |
| | $\frac{h_0}{8}$ | 0.16E-04 | 3.01 | 0.52E-04 | 3.00 |
| | $\frac{h_0}{16}$ | 0.20E-05 | 3.00 | 0.65E-05 | 2.99 |
| $P^1$-limited | $\frac{h_0}{2}$ | 0.61E-01 | - | 0.76E-01 | - |
| | $\frac{h_0}{4}$ | 0.17E-01 | 1.83 | 0.42E-01 | 0.86 |
| | $\frac{h_0}{8}$ | 0.45E-02 | 1.93 | 0.18E-01 | 1.26 |
| | $\frac{h_0}{16}$ | 0.11E-02 | 2.02 | 0.56E-02 | 1.66 |
| $P^2$-limited | $\frac{h_0}{2}$ | 0.33E-02 | - | 0.76E-02 | - |
| | $\frac{h_0}{4}$ | 0.43E-03 | 2.96 | 0.13E-02 | 2.60 |
| | $\frac{h_0}{8}$ | 0.53E-04 | 3.00 | 0.24E-03 | 2.37 |
| | $\frac{h_0}{16}$ | 0.61E-05 | 3.12 | 0.46E-04 | 2.40 |

**TABLE VI**

Accuracy for $u_t + u_x + u_y = 0$ and $u_0(x,y) = sin(\pi(x+y))$. Non-uniform meshes

| Scheme | h | $L^1$-norm | | $L^\infty$-norm | |
|---|---|---|---|---|---|
| | | error | order | error | order |
| $P^1$-unlimited | $\frac{h_0}{2}$ | 0.82E-01 | - | 0.19E+00 | - |
| | $\frac{h_0}{4}$ | 0.17E-01 | 2.27 | 0.42E-01 | 2.15 |
| | $\frac{h_0}{8}$ | 0.37E-02 | 2.19 | 0.92E-02 | 2.19 |
| | $\frac{h_0}{16}$ | 0.86E-03 | 2.11 | 0.23E-02 | 2.00 |
| $P^2$-unlimited | $\frac{h_0}{2}$ | 0.40E-02 | - | 0.13E-01 | - |
| | $\frac{h_0}{4}$ | 0.43E-03 | 3.22 | 0.19E-02 | 2.79 |
| | $\frac{h_0}{8}$ | 0.50E-04 | 3.08 | 0.23E-03 | 3.01 |
| | $\frac{h_0}{16}$ | 0.62E-05 | 3.03 | 0.27E-04 | 3.09 |
| $P^1$-limited | $\frac{h_0}{2}$ | 0.91E-01 | - | 0.19E+00 | - |
| | $\frac{h_0}{4}$ | 0.20E-01 | 2.20 | 0.46E-01 | 2.01 |
| | $\frac{h_0}{8}$ | 0.50E-02 | 1.99 | 0.19E-01 | 1.26 |
| | $\frac{h_0}{16}$ | 0.12E-02 | 2.02 | 0.79E-02 | 1.29 |
| $P^2$-limited | $\frac{h_0}{2}$ | 0.10E-01 | - | 0.24E-01 | - |
| | $\frac{h_0}{4}$ | 0.14E-02 | 2.89 | 0.42E-02 | 2.54 |
| | $\frac{h_0}{8}$ | 0.16E-03 | 3.06 | 0.93E-03 | 2.17 |
| | $\frac{h_0}{16}$ | 0.19E-04 | 3.11 | 0.17E-03 | 2.43 |

**TABLE VII**

**Accuracy for $u_t + u_x + u_y = 0$ and $u_0(x,y) = sin^4(\pi(x+y))$. Uniform**

| | | meshes | | | |
|---|---|---|---|---|---|
| | | $L^1$-norm | | $L^\infty$-norm | |
| Scheme | h | error | order | error | order |
| $P^1$-unlimited | $\frac{h_0}{2}$ | 0.31E+00 | - | 0.26E+00 | - |
| | $\frac{h_0}{4}$ | 0.11E+00 | 1.50 | 0.88E-01 | 1.58 |
| | $\frac{h_0}{8}$ | 0.19E-01 | 2.52 | 0.19E-01 | 2.19 |
| | $\frac{h_0}{16}$ | 0.29E-02 | 2.71 | 0.34E-02 | 2.51 |
| $P^2$-unlimited | $\frac{h_0}{2}$ | 0.64E-01 | - | 0.54E-01 | - |
| | $\frac{h_0}{4}$ | 0.44E-02 | 3.86 | 0.35E-02 | 3.93 |
| | $\frac{h_0}{8}$ | 0.31E-03 | 3.83 | 0.53E-03 | 2.72 |
| | $\frac{h_0}{16}$ | 0.33E-04 | 3.25 | 0.71E-04 | 2.92 |
| $P^1$-limited | $\frac{h_0}{2}$ | 0.39E+00 | - | 0.33E+00 | - |
| | $\frac{h_0}{4}$ | 0.14E+00 | 1.43 | 0.14E+00 | 1.27 |
| | $\frac{h_0}{8}$ | 0.33E-01 | 2.12 | 0.52E-01 | 1.40 |
| | $\frac{h_0}{16}$ | 0.77E-02 | 2.10 | 0.19E-01 | 1.42 |
| $P^2$-limited | $\frac{h_0}{2}$ | 0.15E+00 | - | 0.14E+00 | - |
| | $\frac{h_0}{4}$ | 0.27E-01 | 2.43 | 0.36E-01 | 1.94 |
| | $\frac{h_0}{8}$ | 0.42E-02 | 2.69 | 0.87E-02 | 2.05 |
| | $\frac{h_0}{16}$ | 0.34E-03 | 3.62 | 0.96E-03 | 3.17 |

**TABLE VIII**

Accuracy for $u_t + u_x + u_y = 0$ and $u_0(x, y) = sin^4(\pi(x + y))$. Non-

uniform meshes

| Scheme | h | $L^1$-norm | | $L^\infty$-norm | |
|---|---|---|---|---|---|
| | | error | order | error | order |
| $P^1$-unlimited | $\frac{h_0}{2}$ | 0.55E+00 | - | 0.51E+00 | - |
| | $\frac{h_0}{4}$ | 0.20E+00 | 1.46 | 0.25E+00 | 1.02 |
| | $\frac{h_0}{8}$ | 0.52E-01 | 1.92 | 0.84E-01 | 1.60 |
| | $\frac{h_0}{16}$ | 0.85E-02 | 2.62 | 0.17E-01 | 2.33 |
| $P^2$-unlimited | $\frac{h_0}{2}$ | 0.18E+00 | - | 0.21E+00 | - |
| | $\frac{h_0}{4}$ | 0.24E-01 | 2.90 | 0.37E-01 | 2.54 |
| | $\frac{h_0}{8}$ | 0.14E-02 | 4.11 | 0.28E-02 | 3.70 |
| | $\frac{h_0}{16}$ | 0.11E-03 | 3.65 | 0.39E-03 | 2.84 |
| $P^1$-limited | $\frac{h_0}{2}$ | 0.59E+00 | - | 0.54E+00 | - |
| | $\frac{h_0}{4}$ | 0.21E+00 | 1.48 | 0.26E+00 | 1.03 |
| | $\frac{h_0}{8}$ | 0.54E-01 | 1.96 | 0.83E-01 | 1.66 |
| | $\frac{h_0}{16}$ | 0.11E-01 | 2.29 | 0.21E-01 | 1.97 |
| $P^2$-limited | $\frac{h_0}{2}$ | 0.23E+00 | - | 0.27E+00 | - |
| | $\frac{h_0}{4}$ | 0.43E-01 | 2.45 | 0.75E-01 | 1.82 |
| | $\frac{h_0}{8}$ | 0.67E-02 | 2.67 | 0.14E-01 | 2.39 |
| | $\frac{h_0}{16}$ | 0.82E-03 | 3.03 | 0.30E-02 | 2.24 |

**TABLE IX**

**Accuracy for the vortex advection. Uniform meshes**

| Scheme | h | $L^1$-norm | | $L^\infty$-norm | |
|---|---|---|---|---|---|
| | | error | order | error | order |
| $P^1$-unlimited | $\frac{h_0}{2}$ | 0.93E-02 | - | 0.20E+00 | - |
| | $\frac{h_0}{4}$ | 0.25E-02 | 1.92 | 0.48E-01 | 2.07 |
| | $\frac{h_0}{8}$ | 0.55E-03 | 2.17 | 0.11E-01 | 2.11 |
| | $\frac{h_0}{16}$ | 0.12E-03 | 2.13 | 0.30E-02 | 1.91 |
| $P^2$-unlimited | $\frac{h_0}{2}$ | 0.16E-02 | - | 0.18E-01 | - |
| | $\frac{h_0}{4}$ | 0.25E-03 | 2.64 | 0.53E-02 | 1.77 |
| | $\frac{h_0}{8}$ | 0.29E-04 | 3.13 | 0.69E-03 | 2.94 |
| | $\frac{h_0}{16}$ | 0.31E-05 | 3.20 | 0.92E-04 | 2.91 |
| $P^1$-limited | $\frac{h_0}{2}$ | 0.98E-02 | - | 0.22E+00 | - |
| | $\frac{h_0}{4}$ | 0.29E-02 | 1.78 | 0.61E-01 | 1.86 |
| | $\frac{h_0}{8}$ | 0.72E-03 | 1.98 | 0.18E-01 | 1.74 |
| | $\frac{h_0}{16}$ | 0.18E-03 | 1.97 | 0.69E-02 | 1.40 |
| $P^2$-limited | $\frac{h_0}{2}$ | 0.63E-02 | - | 0.12E+00 | - |
| | $\frac{h_0}{4}$ | 0.10E-02 | 2.60 | 0.24E-01 | 2.29 |
| | $\frac{h_0}{8}$ | 0.83E-04 | 3.64 | 0.23E-02 | 3.34 |
| | $\frac{h_0}{16}$ | 0.77E-05 | 3.44 | 0.33E-03 | 2.85 |

**TABLE X**

Accuracy for the vortex advection. Non-uniform meshes

| Scheme | h | $L^1$-norm | | $L^\infty$-norm | |
| --- | --- | --- | --- | --- | --- |
| | | error | order | error | order |
| $P^1$-unlimited | $\frac{h_0}{2}$ | 0.78E-02 | - | 0.13E+00 | - |
| | $\frac{h_0}{4}$ | 0.21E-02 | 1.87 | 0.49E-01 | 1.40 |
| | $\frac{h_0}{8}$ | 0.49E-03 | 2.13 | 0.11E-01 | 2.17 |
| | $\frac{h_0}{16}$ | 0.12E-03 | 2.07 | 0.31E-02 | 1.78 |
| $P^2$-unlimited | $\frac{h_0}{2}$ | 0.16E-02 | - | 0.28E-01 | - |
| | $\frac{h_0}{4}$ | 0.23E-03 | 2.76 | 0.60E-02 | 2.24 |
| | $\frac{h_0}{8}$ | 0.28E-04 | 3.04 | 0.77E-03 | 2.96 |
| | $\frac{h_0}{16}$ | 0.32E-05 | 3.15 | 0.10E-03 | 2.96 |
| $P^1$-limited | $\frac{h_0}{2}$ | 0.94E-02 | - | 0.20E+00 | - |
| | $\frac{h_0}{4}$ | 0.29E-02 | 1.71 | 0.65E-01 | 1.61 |
| | $\frac{h_0}{8}$ | 0.73E-03 | 1.97 | i0.23E-01 | 1.53 |
| | $\frac{h_0}{16}$ | 0.18E-03 | 2.02 | 0.89E-02 | 1.35 |
| $P^2$-limited | $\frac{h_0}{2}$ | 0.81E-02 | - | 0.13E+00 | - |
| | $\frac{h_0}{4}$ | 0.12E-02 | 2.72 | 0.26E-01 | 2.33 |
| | $\frac{h_0}{8}$ | 0.11E-03 | 3.48 | 0.26E-02 | 3.30 |
| | $\frac{h_0}{16}$ | 0.14E-04 | 3.01 | 0.46E-03 | 2.50 |
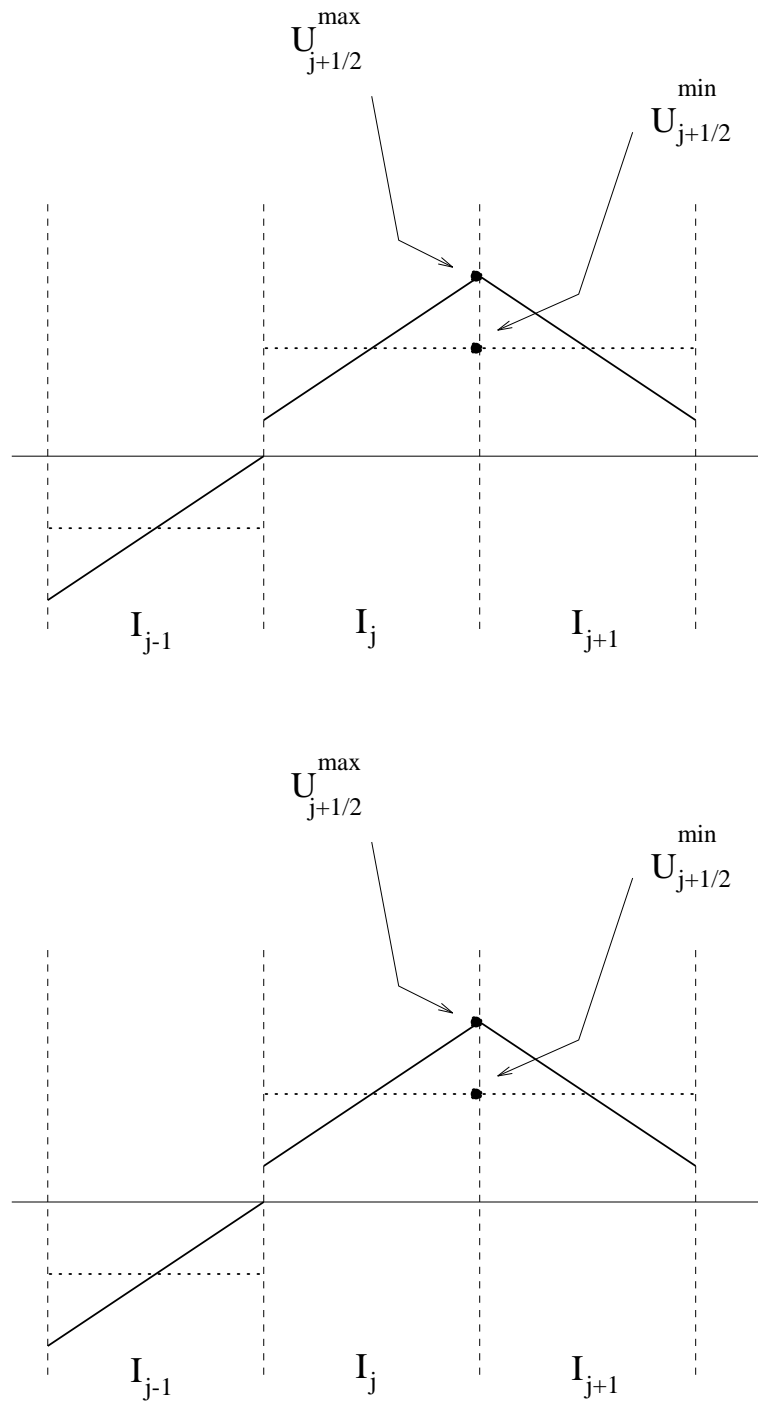
**FIG. 1.** Effects of slope limiters for a smooth (top) and a non-smooth (bottom) extremum, for piecewise linear RKDG methods; the proposed limiter (designed by max) and the Biswas *et al.* limiter (min) act differently for a smooth extremum
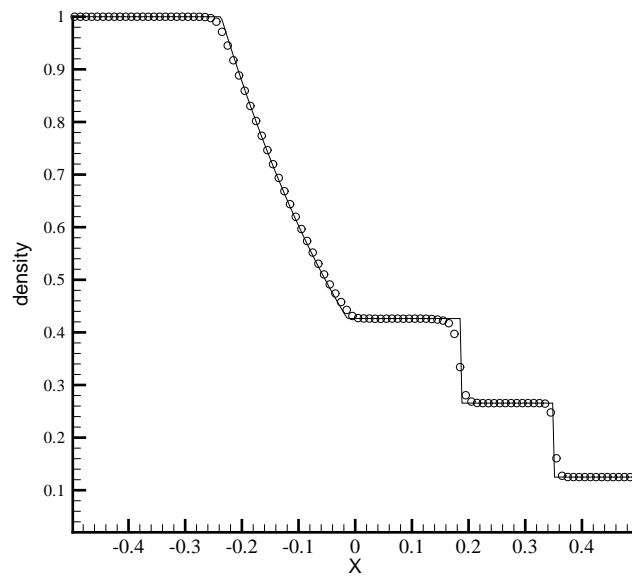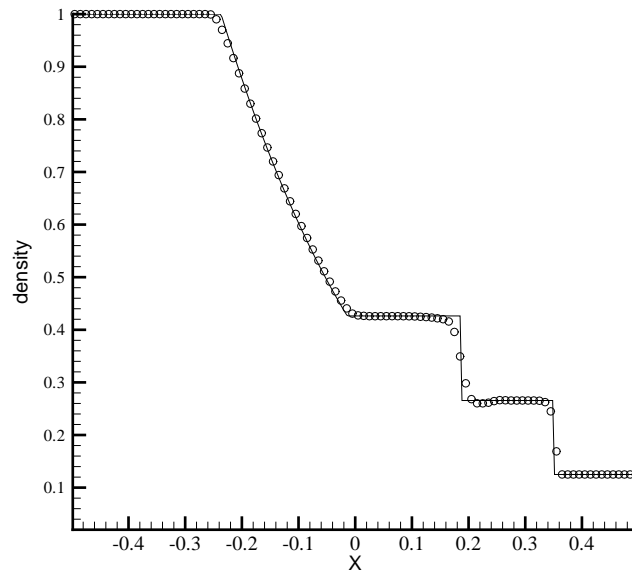
**FIG. 2.** Sod shock-tube problem. 100 points. The resulting density contours of employing the new limiter, exact solution (solid line), approximate solution (o). Second-order (top) and third-order (bottom) approximations

52
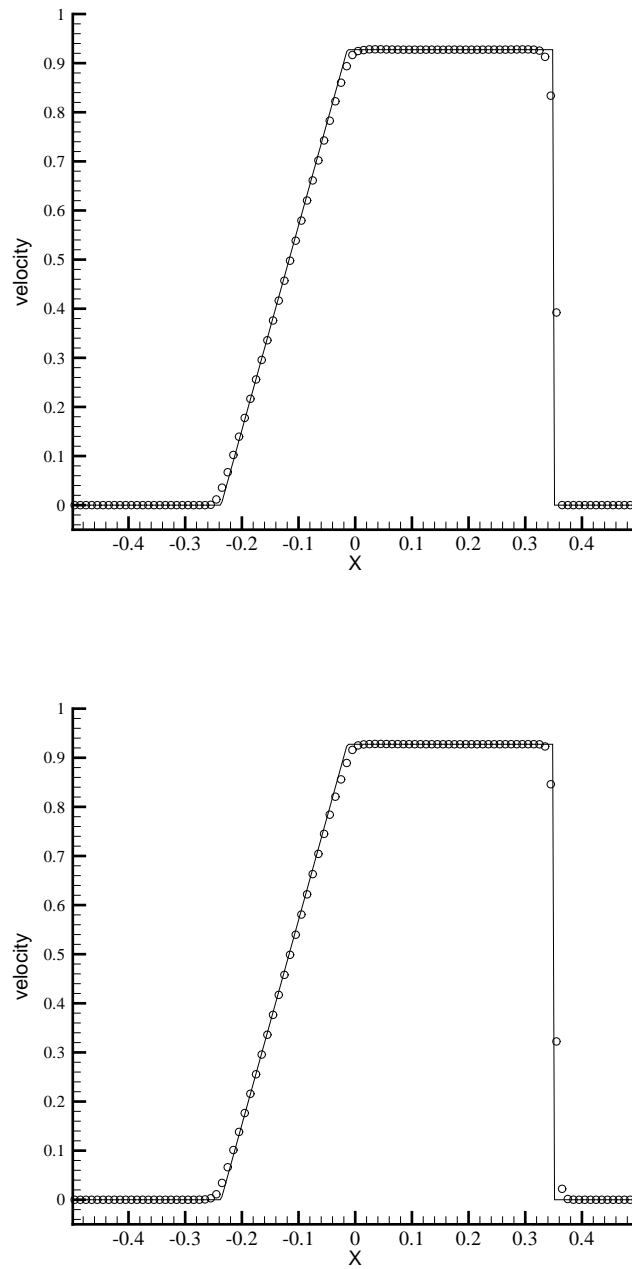


**FIG. 3.** Sod shock-tube problem. 100 points. The resulting velocity contours of employing the new limiter, exact solution (solid line), approximate solution (o). Second-order (top) and third-order (bottom) approximations
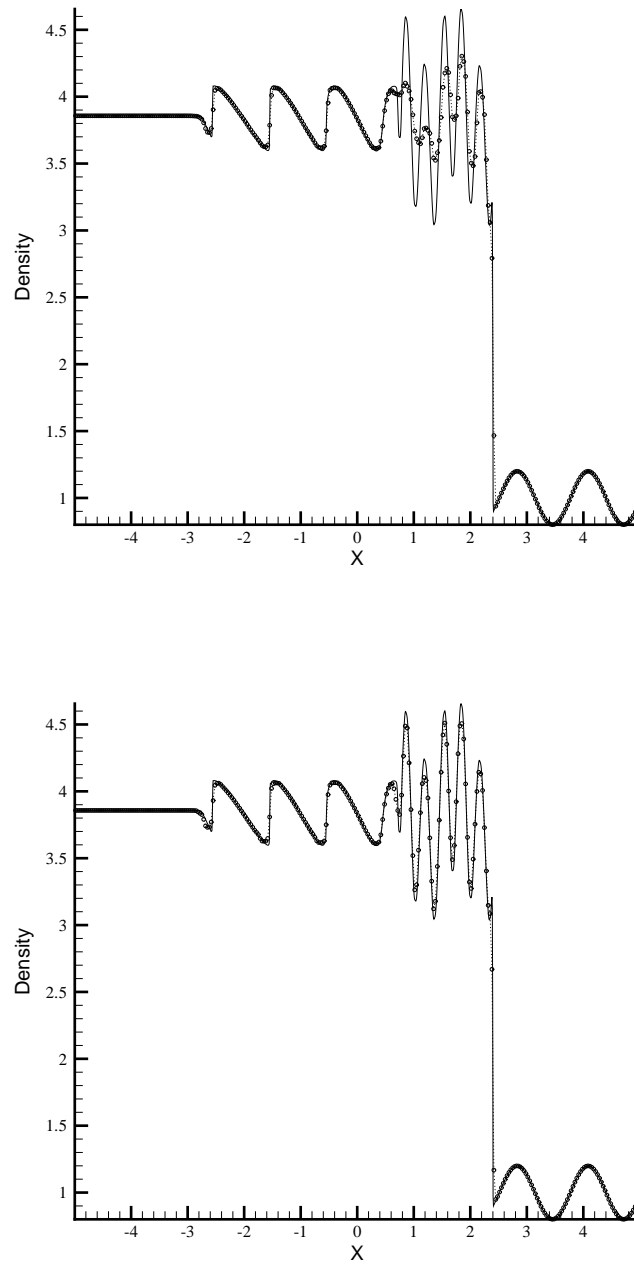
**FIG. 4.** Shu and Osher's test case. The resulting density contours of employing the new limiter. 300 points. Exact solution (solid line), second-order $P^1$ (top) and third-order $P^2$ (bottom) approximate solutions (○)
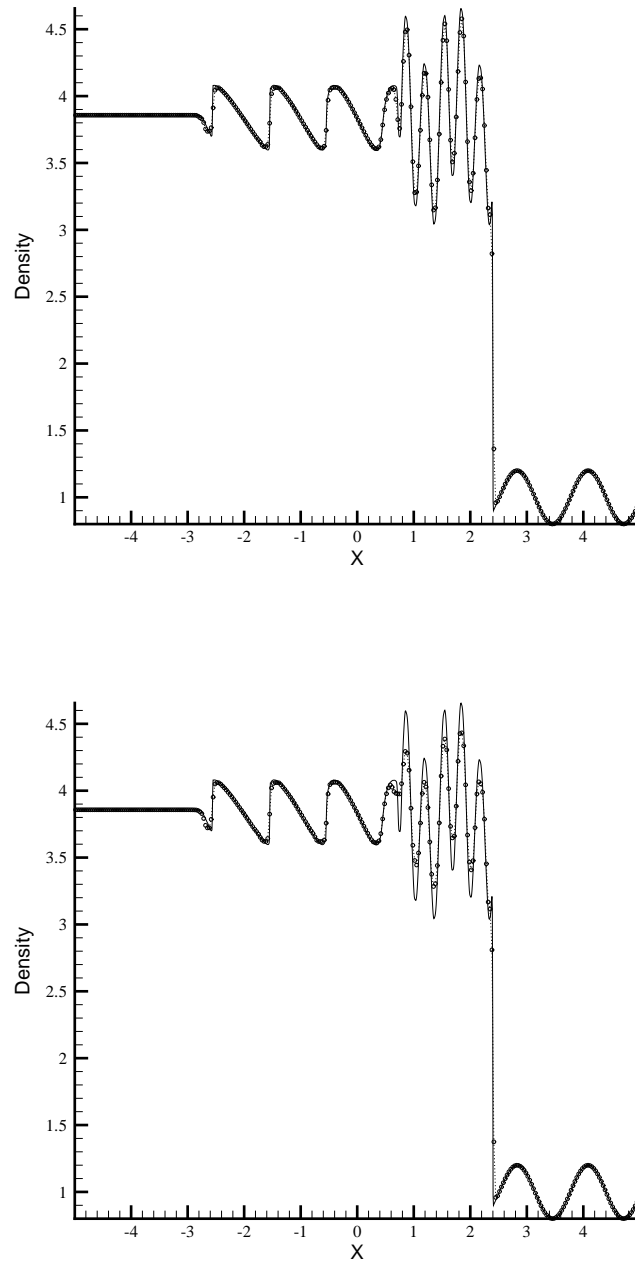
**FIG. 5.**    Shu and Osher's test case. 300 points. Exact solution (solid line) and fourth-order $P^3$ approximate solution (○). The resulting density contours of employing the new limiter (top) and the Biswas *et al.* limiter (bottom)
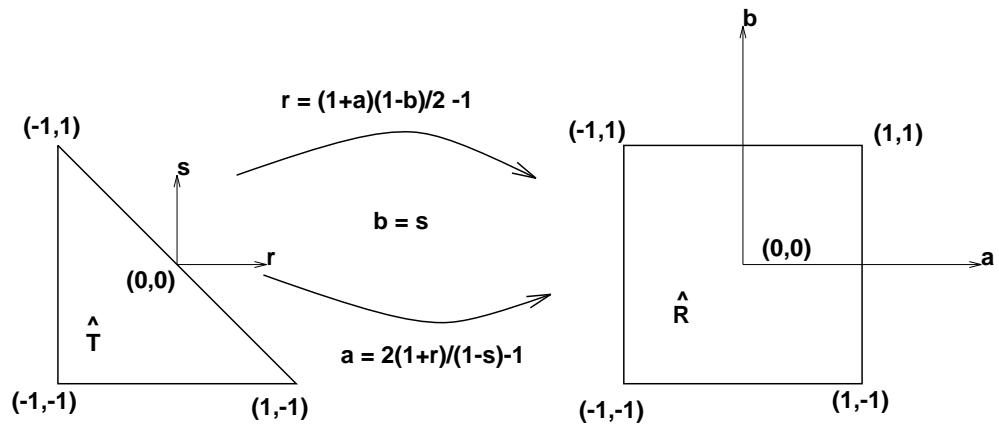
**FIG. 6.** Transforms between standard triangle $\hat{T}$ and standard quadrilateral $\hat{Q}$.
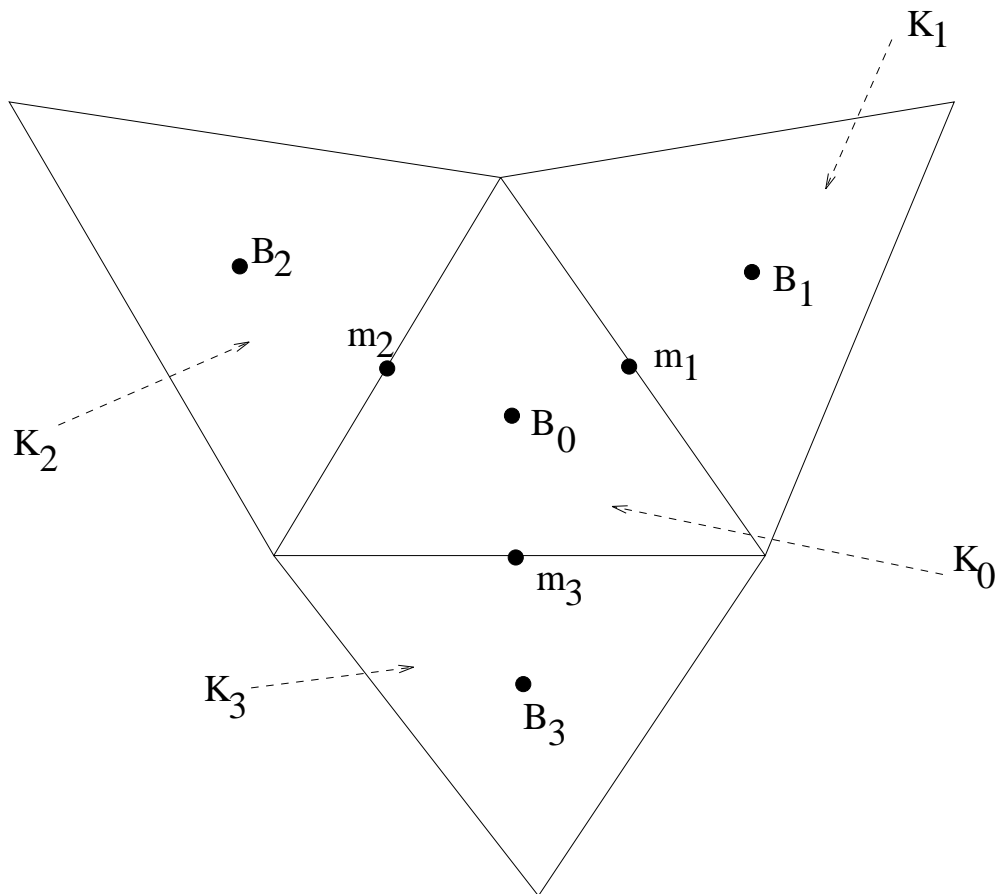
**FIG. 7.** Notations for the neighbours of the triangle $K_0$
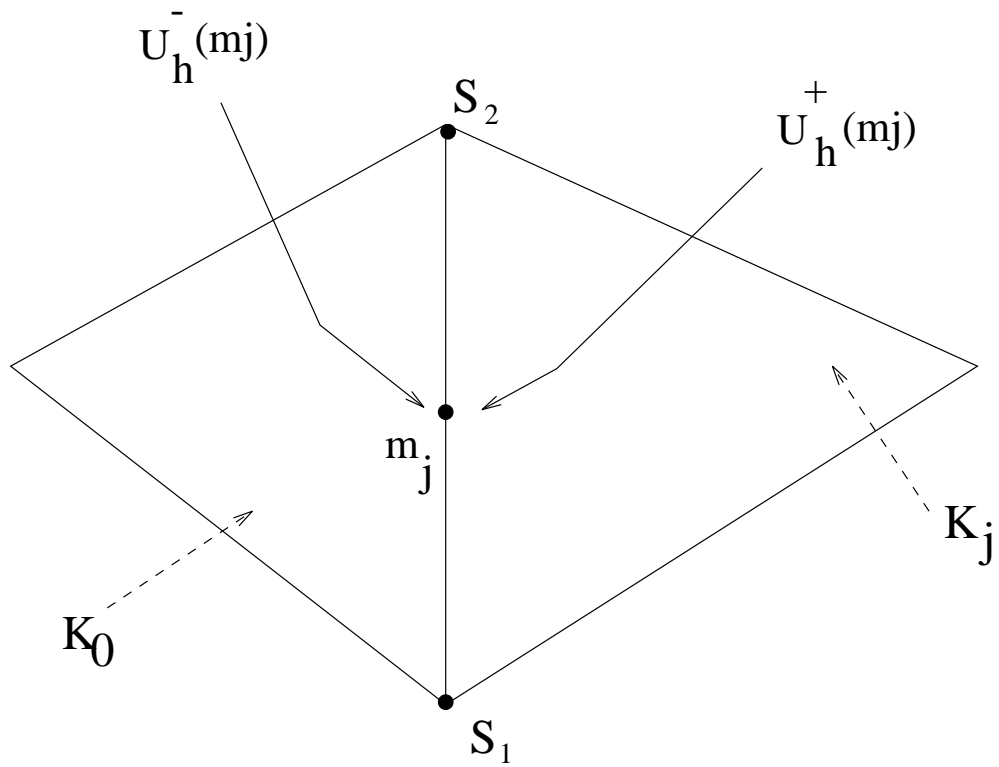
**FIG. 8.** Notations for the approximate solution on interface $j$
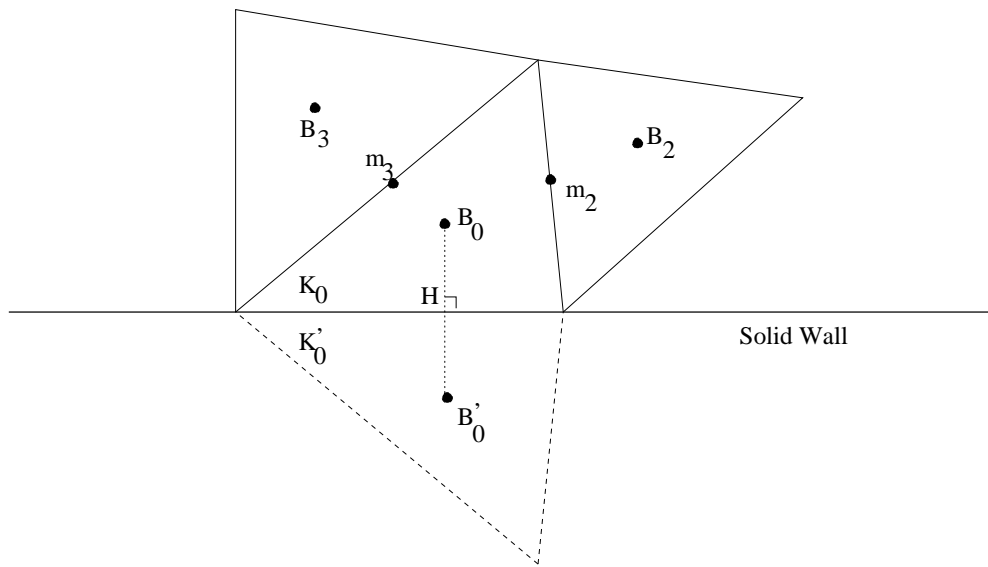
**FIG. 9.** Notations for the limiting procedure at solid walls
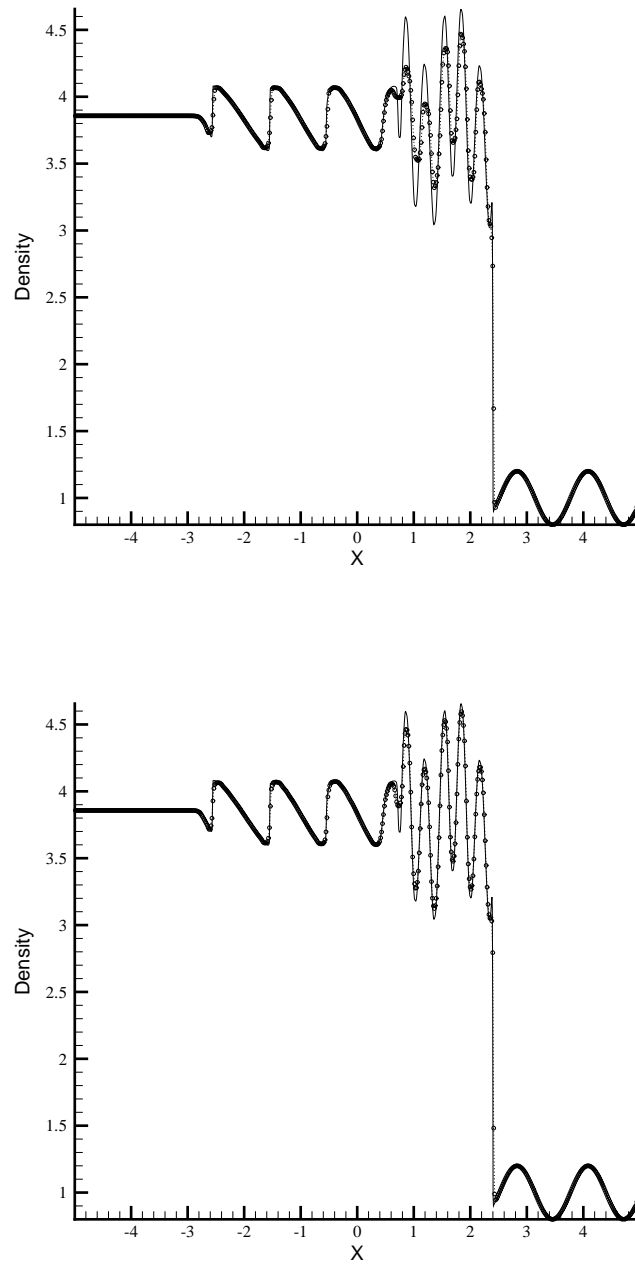
**FIG. 10.** Shu and Osher's test case. The resulting density contours of employing the new limiter defined for the two-dimensionnal method. Second-order $P^1$ (top) and third-order $P^2$ (bottom) approximate solutions. 300 points in the direction of the flow field
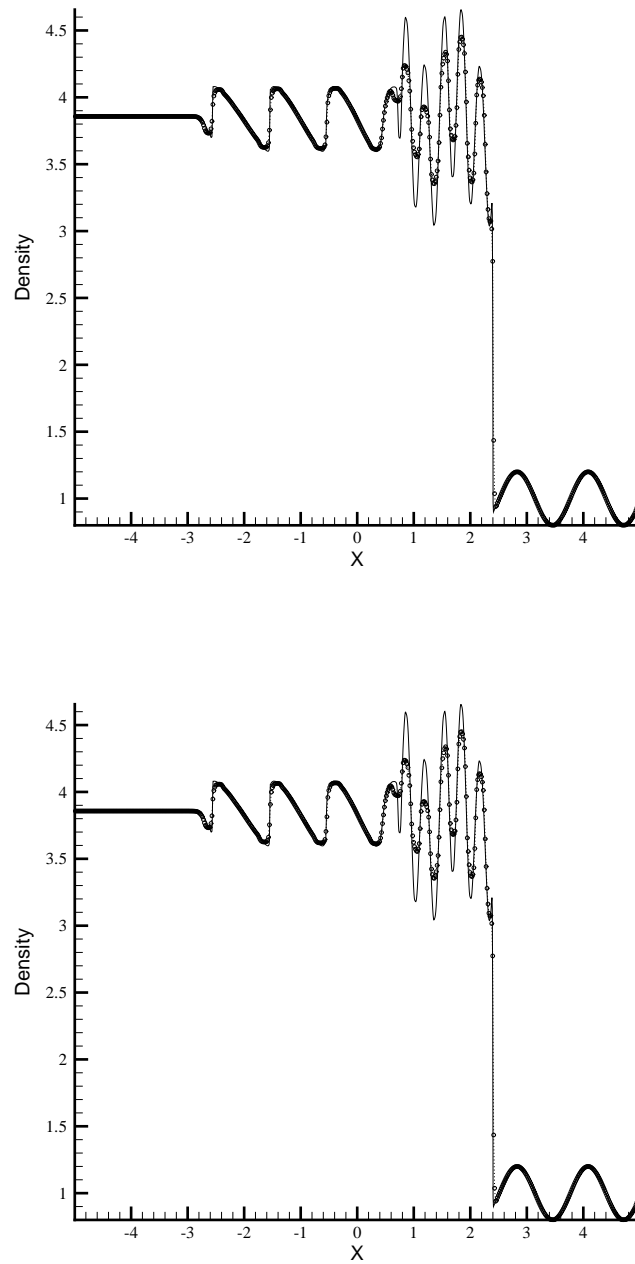
**FIG. 11.** Shu and Osher's test case. A third-order $P^2$ approximate solution in regions of regularity and second-order $P^1$ approximation near solution discontinuities (top) and a $P^2$ approximate solution without applying the regularity criterion (bottom). Two-dimensional solution, 300 points in the direction of the flow field
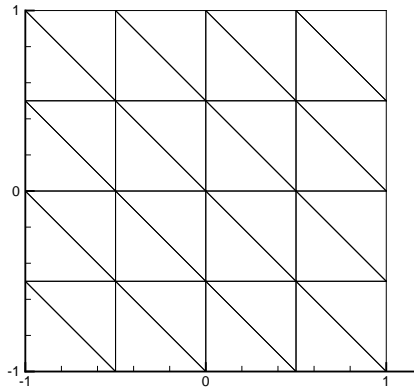
**FIG. 12.** The coarsest uniform mesh for test accuracy with the linear transport equation
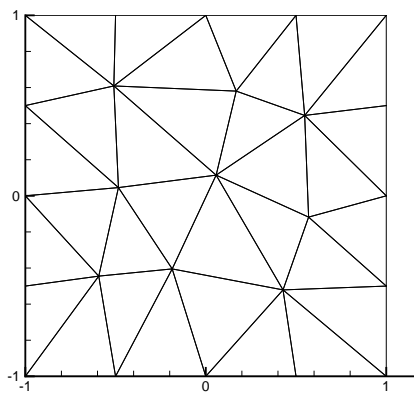


**FIG. 13.** The coarsest nonuniform mesh for test accuracy with the linear transport equation
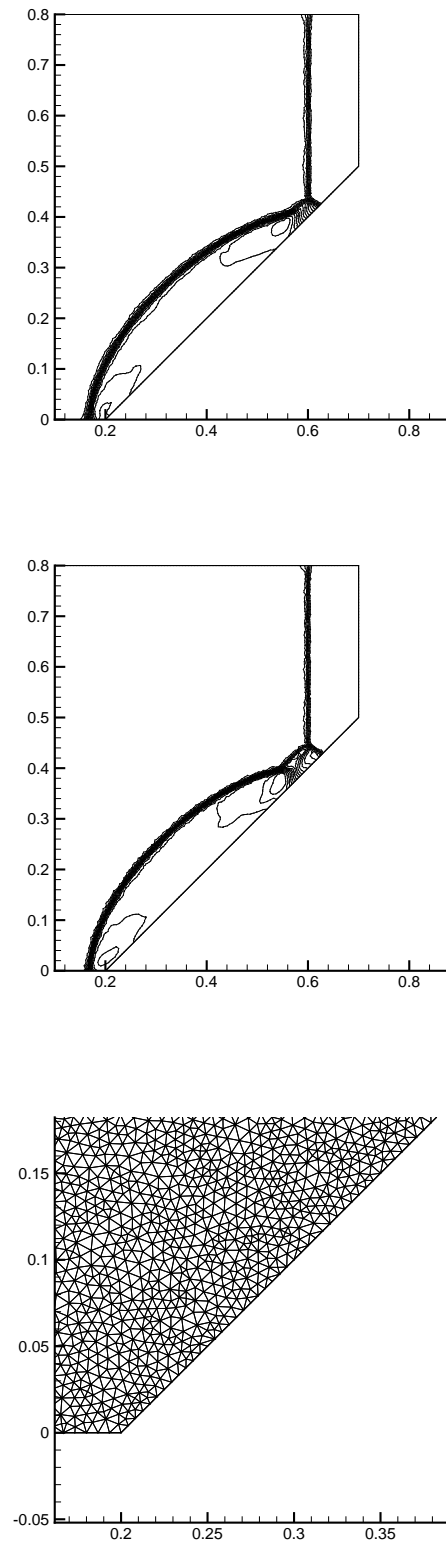
**FIG. 14.**   Reflection of a plane shock from a ramp.   Second-order $P^1$ results with the minmod limiter (top) and the new one (middle). A 20 511 triangle mesh (bottom). Density $\rho$ : 20 equally spaced contour lines from $\rho = 2.56$ to $\rho = 19$.
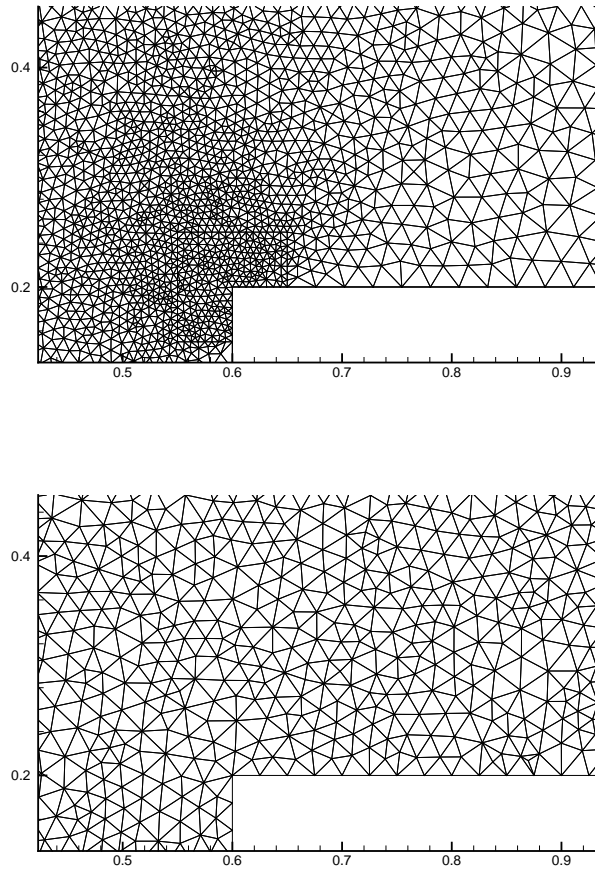
**FIG. 15.** Forward-facing step problem. Detail of the triangulations around the corner. Mesh A contains 13774 triangles (top). Mesh B contains 14392 (bottom).
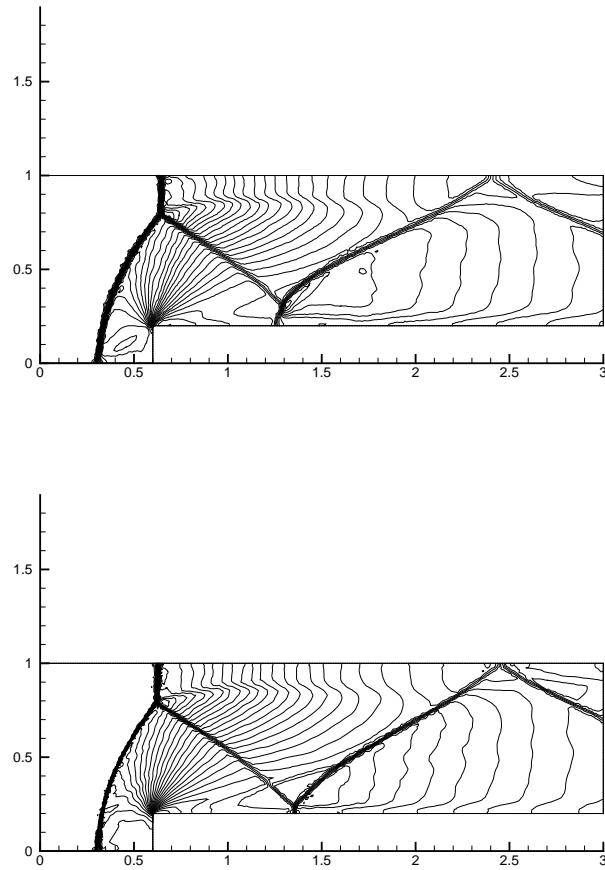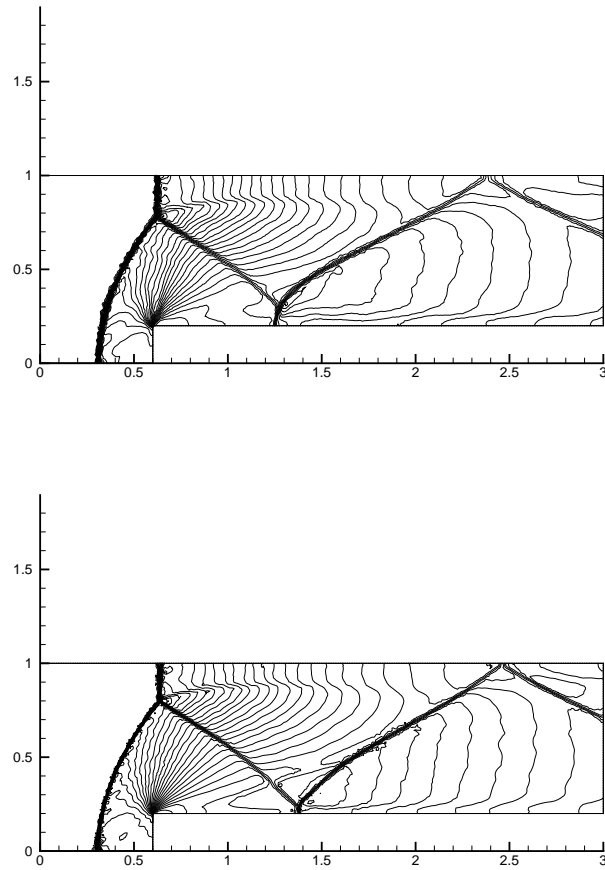
**FIG. 16.**   Forward-facing step problem. Second-order $P^1$ results with mesh A (top) and mesh B (bottom). Density $\rho$ : 30 equally spaced contour lines from $\rho = 0.090338$ to $\rho = 6.2365$.
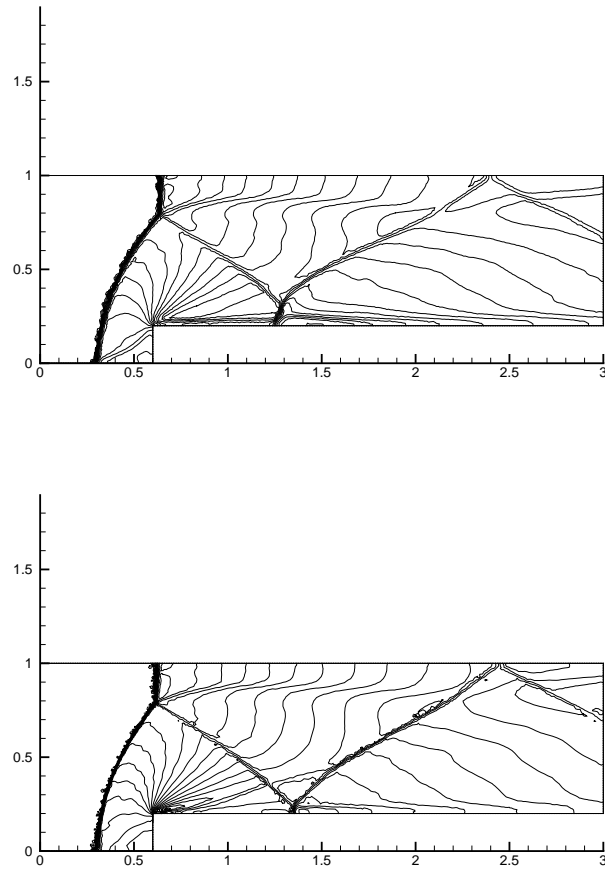
**FIG. 17.**    Forward-facing step problem. Second-order $P^1$ results with mesh A (top) and mesh B (bottom). Mach number : 25 equally spaced contour lines from 0.02 to 3.82.

66
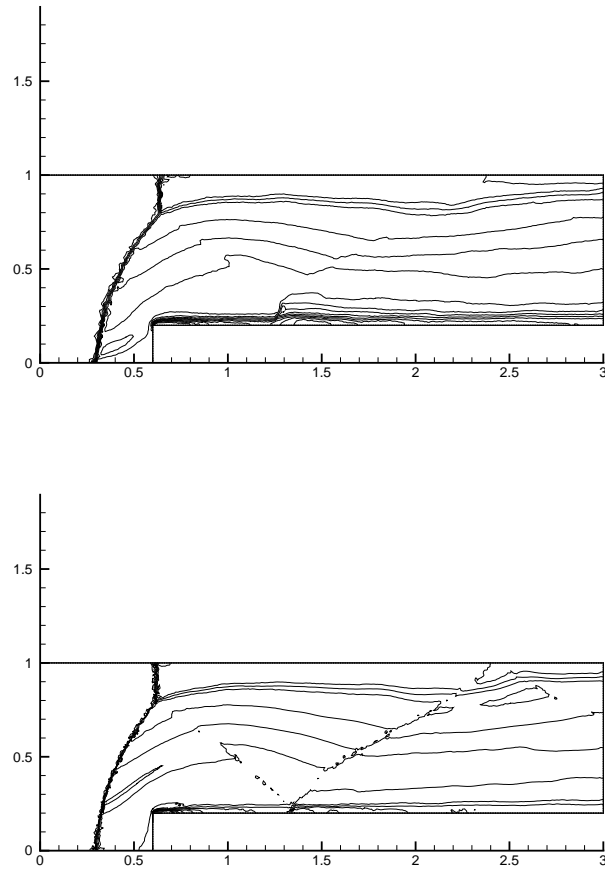


**FIG. 18.** Forward-facing step problem. Second-order $P^1$ results with mesh A (top) and mesh B (bottom). Entropy production near the step corner : 17 equally spaced contour lines from 0.63 to 1.5.
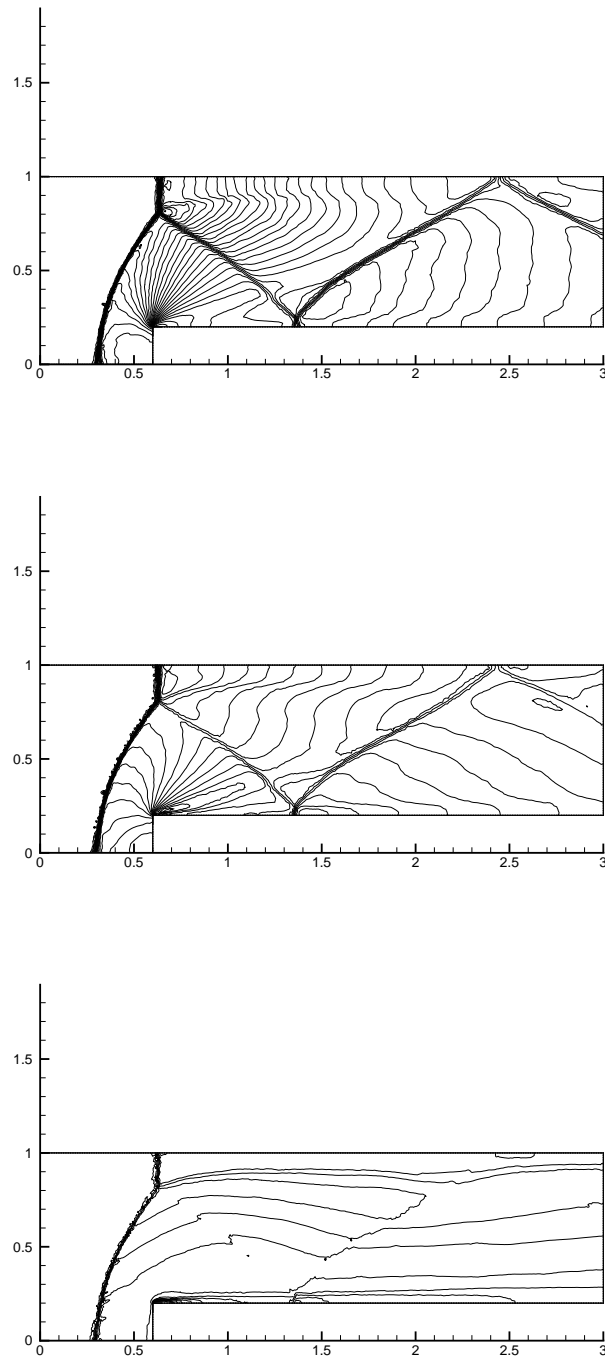
**FIG. 19.** Forward-facing step problem. Second-order $P^1$ results with the minmod limiter and mesh B. Density $\rho$ : 30 equally spaced contour lines from $\rho = 0.090338$ to $\rho = 6.2365$ (top). Mach number : 25 equally spaced contour lines from 0.02 to 3.82 (middle). Entropy production near the step corner : 17 equally spaced contour lines from 0.63 to 1.5 (bottom).

**FIG. 20.** Forward-facing step problem. Third-order $P^2$ results with mesh A (top) and mesh B (bottom). Density $\rho$ : 30 equally spaced contour lines from $\rho = 0.090338$ to $\rho = 6.2365$.
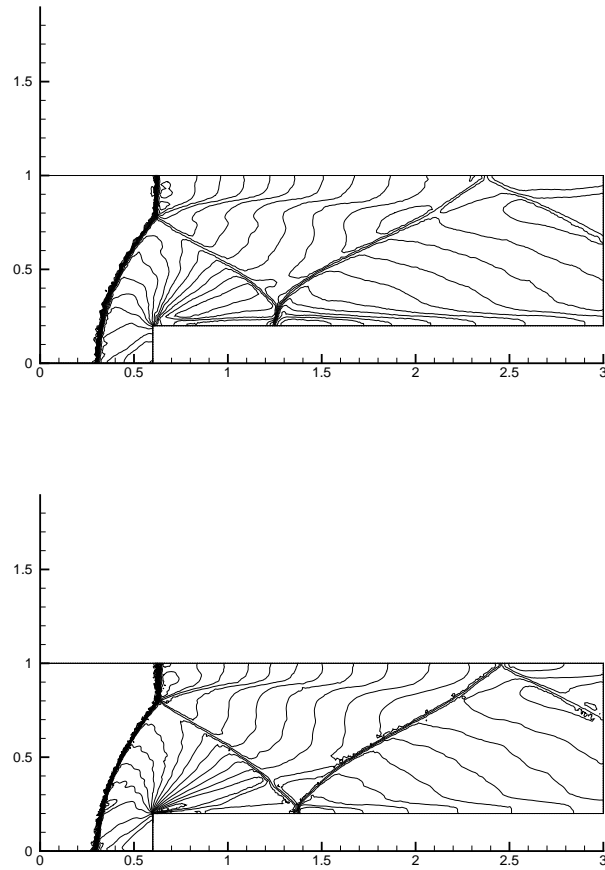
**FIG. 21.** Forward-facing step problem. Third-order $P^2$ results with mesh A (top) and mesh B (bottom). Mach number : 25 equally spaced contour lines from 0.02 to 3.82.
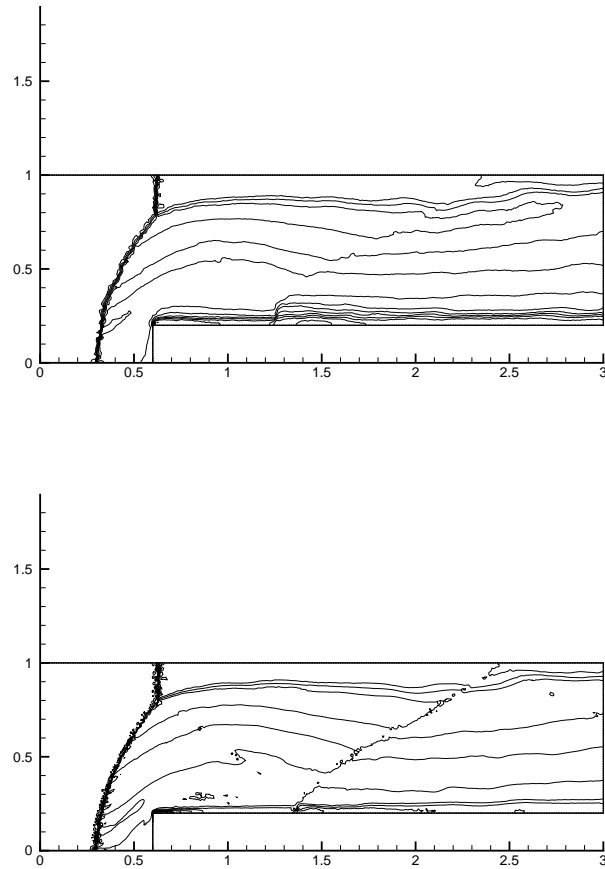
**FIG. 22.**    Forward-facing step problem. Third-order $P^2$ results with mesh A (top) and mesh B (bottom). Entropy production near the step corner : 17 equally spaced contour lines from 0.63 to 1.5.
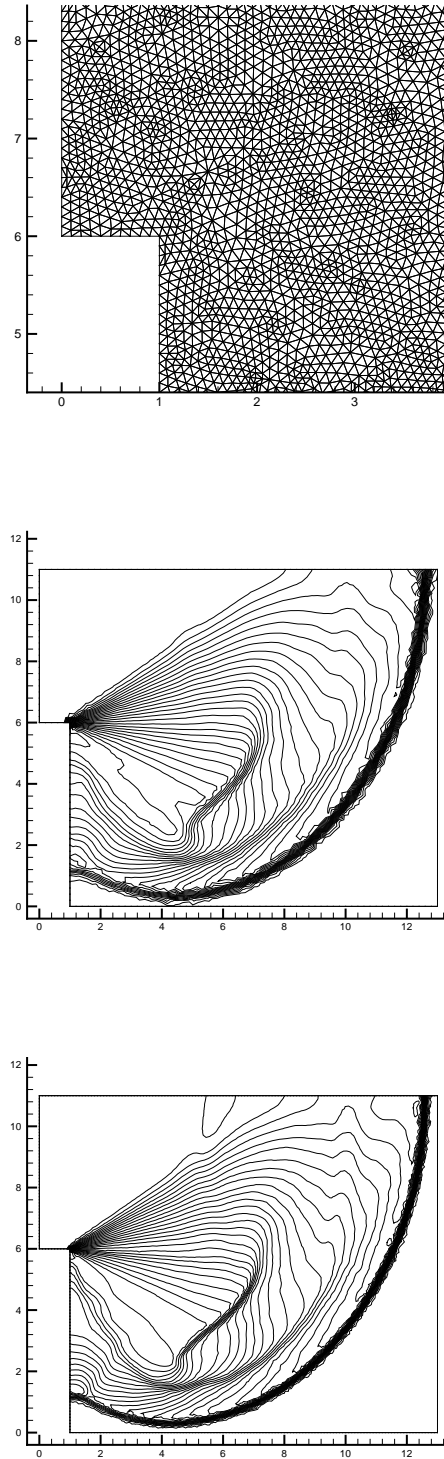
**FIG. 23.**    Shock passing a backward-facing corner. Details of the triangulation around the corner for the coarse mesh (top). Third-order $P^2$ results with new limiter on the coarse mesh (middle) and the fine one (bottom). Density $\rho$ : 25 equally spaced contour lines from $\rho = 0.066$ to $\rho = 7.06$.